Title

Enhanced mitochondrial inhibition by 3,4-dihydroxyphenyl-acetaldehyde (DOPAL)-oligomerized α-synuclein

Journal

Journal of Neuroscience Research, 97(12)

ISSN

0360-4012

Authors

Sarafian, Theodore A

Yacoub, Amneh

Kunz, Anastasia

et al.

Publication Date

2019-12-01

DOI

10.1002/jnr.24513

Peer reviewed

HHS Public Access

Author manuscript

J Neurosci Res. Author manuscript; available in PMC 2020 December 01.

Published in final edited form as:

J Neurosci Res. 2019 December ; 97(12): 1689–1705. doi:10.1002/jnr.24513.

Enhanced Mitochondrial Inhibition by 3,4-Dihydroxyphenyl-Acetaldehyde (DOPAL)-Oligomerized α-Synuclein

Theodore A. Sarafian, **Amneh Yacoub**, **Anastasia Kunz**, **Burkan Aranki**, **Grigor Serobyan**, **Whitaker Cohn**, **Julian P Whitelegge**, **Joseph B. Watson**

Department of Psychiatry & Biobehavioral Sciences, David Geffen School of Medicine at UCLA, UCLA, Los Angeles, CA

Abstract

Oligomeric forms of α-synuclein are believed to cause mitochondrial injury, which may contribute to neurotoxicity in Parkinson's disease (PD). Here oligomers of α-synuclein were prepared using the dopamine metabolite, DOPAL (3,4-dihydroxyphenyl-acetaldehyde), in the presence of guanidinium hydrochloride. Electron microscopy, mass spectrometry and Western blotting studies revealed enhanced and stable oligomerization with DOPAL compared with dopamine or $CuCl_2/H_2O_2$. Using isolated mouse brain mitochondria, DOPAL-oligomerized α-synuclein (DOS) significantly inhibited oxygen consumption rates compared with untreated, control-fibrillated, and dopamine-fibrillated synuclein, or with monomeric α-synuclein. Inhibition was greater in the presence of malate plus pyruvate than with succinate, suggesting the involvement of mitochondrial complex I. Mitochondrial membrane potential studies using fluorescent probes, JC-1 and Safranin O, also detected enhanced inhibition by DOS compared with the other aggregated forms of α-synuclein. Testing a small customized chemical library, four compounds were identified that rescued membrane potential from DOS injury. While diverse in chemical structure and mechanism, each compound has been reported to interact with mitochondrial complex I. Western blotting studies revealed that none of the four compounds disrupted the oligomeric banding pattern of DOS, suggesting their protection involved direct mitochondrial interaction. The remaining set of chemicals also did not disrupt oligomeric banding, attesting to the high structural stability of this α-synuclein proteoform. DOPAL and α-synuclein are both found in dopaminergic neurons, where their levels are elevated in PD and in animal models exposed to chemical toxicants, including agricultural pesticides. The current study provides further evidence of α-synuclein-induced mitochondrial injury and a likely role in PD neuropathology.

Graphical Abstract

To whom correspondence should be addressed: Joseph B. Watson, Ph.D., Semel Institute for Neuroscience and Human Behavior, Room 58-258B, David Geffen School of Medicine at UCLA, 760 Westwood Plaza, Los Angeles, CA 90095-1759, Phone (310)-825-7587; Fax (310)-206-5060; jwatson@mednet.ucla.edu.

ROLE OF AUTHORS

All authors had full access to all of the data in the study and take responsibility for the integrity and the accuracy of the data analysis. Conceptualization: T.A.S., J.B.W. Methodology, Investigation, Analysis, Resources: T.A.S., J.B.W, J.P.W., A.Y., A.K., B.A., G.S., W.C.Writing: T.A.S., J.B.W. Supervision: J.B.W., T.A.S.

CONFLICT OF INTEREST STATEMENT

We are not aware of any conflicts of interests of any kind by the listed authors, who contributed to this manuscript's collective work.

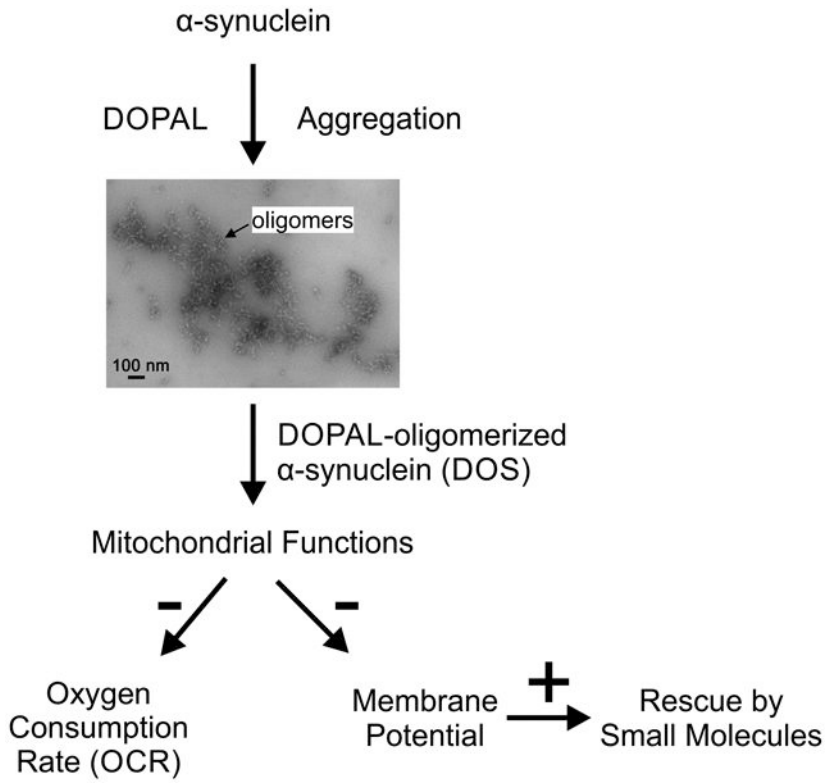

Keywords

α-synuclein oligomers; DOPAL; oxygen consumption rate; mitochondrial membrane potential; small molecule rescue; RRIDs: Antibodies (AB_398107; AB_437779); Software (RRID: SCR_003210)

INTRODUCTION

For decades, dopamine metabolism has been considered a central factor underlying the selective vulnerability of dopaminergic neurons of the pars compacta in the substantia nigra (SN) of Parkinson's disease (PD) patients (Stokes et al., 1999; Dauer and Przedborski, 2003; Houlden and Singleton, 2012). The neurochemical buildup of dopamine's oxidation products in these neurons together with their unique physiological and anatomical properties may create a deadly cellular cocktail in PD (Mor and Ischiropoulos, 2018; Post et al., 2018). With the discovery that Lewy bodies, the major hallmarks of PD, contain mainly aggregated α-synuclein, a likely additional toxic trigger for SN dopaminergic neurons is one or more soluble proteoforms of α-synuclein (Roberts and Brown, 2015).

One of the major challenges in the study of α-synuclein aggregates has been the dynamic instability of the various oligomeric and fibrillar forms that can be generated experimentally (Luth et al., 2015; Bose and Beal, 2016; Cremades et al., 2017; Ammal Kaidery and Thomas, 2018, Joshi and Mochly-Rosen, 2018). Remarkably, both dopamine and its aldehyde product of monoamine oxidase, 3,4-dihydroxyphenyl-acetaldehyde (DOPAL),

preferentially produce α-synuclein oligomers at the expense of amyloid fibrils in both cellular and cell-free models (Conway et al., 2001; Mazzulli et al., 2006; Follmer et al., 2007; Follmer et al., 2015; Werner-Allen et al., 2016; Plotegher et al., 2017; Werner-Allen et al., 2018). This is noteworthy, since the oligomeric forms of α-synuclein are the likely main toxic proteoforms in PD (Winner et al., 2011; Villar-Pique et al., 2015). Thus excessive buildup of either dopamine or DOPAL, for example due to environmental and metabolic insults (Norris et al., 2005; Fitzmaurice et al., 2013; Luth et al., 2014; Fischer and Matera, 2015), could in principle lead to the accumulation of α-synuclein oligomers.

Along with deficits in dopamine metabolism, mitochondrial impairment remains a major area of research interest in PD (Kones, 2010; Helley et al., 2017). Both environmental insults such as chronic pesticide exposure and multiple genetic mutations associated with familial PD, including α-synuclein, parkin, PTEN-induced putative kinase 1 (PINK1), DJ-1, leucine-rich repeat kinase 2 (LRRK2), ATPase 13A2 (ATP13A2) and the vacuolar protein sorting associated protein 35 (VPS36), have been associated with impaired mitochondrial function (Grunewald et al., 2018). In the case of α-synuclein, both single-base mutations and overexpressed forms of the protein disrupted multiple mitochondrial targets including membrane potential, complex I, ATP synthase, VDAC, and TOM 20 (Devi et al., 2008; Sarafian et al., 2013; Subramaniam et al., 2014; Rostovtseva et al., 2015; Di Maio et al., 2016; Ludtmann et al., 2018). A common theme that has emerged from these collective studies is the principal toxicity of the oligomeric forms of α-synuclein.

In this study, a novel method was used to enhance production of α-synuclein oligomers by co-incubating α-synuclein with DOPAL and guanidinium hydrochloride (GdnCl) (Sarafian et al., 2017). A cell-free preparation of isolated mouse forebrain mitochondria displayed both diminished oxygen consumption rate (OCR) and membrane potentials upon exposure to DOPAL-oligomerized synuclein (DOS). Dopamine-aggregated α-synuclein was less inhibitory and $CuCl_2/H_2O_2$ oxidized, control-fibrillated, and monomeric α-synuclein were not toxic in these assays. Since mitochondrial injury is a key feature of PD, a variety of commercially available, small molecule agents were also tested for their ability to counteract the mitochondrial injury caused by DOS.

MATERIALS AND METHODS

Animals

WT animals included either C57BL/6 (RRID, IMSR_JAX:000664) or B6CBA (RRID, IMSR JAX: 100011) mice (Sarafian et al., 2017). On average, an equal number of male and female mice were used and ranged in age from 2-5 months. No significant differences were observed in multiple assays (e.g. see Membrane Potential and OCR below) in male versus female mice. Groups of 3-4 animals were maintained in cages on a 12 h light cycle at room temperature (21oC) and were fed food and water *ad libitum*. All efforts were made to minimize the number of animals used. Animals were anesthetized with isoflurane prior to dissecting out forebrain tissue. Forebrain (~1.0-2.0 mg) samples were divided into two sections along the central commissure for mitochondrial preparations. Studies were carried out according to guidelines of the National Institutes of Health Guide for Care and Use of Laboratory Animals (NIH Publications No. 80-23), “Guidelines for the Use of Animals in

Neuroscience Research" (Society for Neuroscience), and with approval from the Institutional Animal Care and Use Committee at UCLA.

Antibodies/Reagents/Recombinant Proteins

Antibodies: A mouse monoclonal antibody raised against rat α-synuclein (aa 15-123 immunogen, 1:2000 dilution, Clone 42, BD Transduction Laboratories™, San Jose, CA) (RRID: AB_398107) was used. Secondary antibody was anti-mouse (RRID: AB_437779) conjugated to horseradish peroxidase (HRP, 1:2500 dilution)(CalBiochem/MilliporeSigma, San Diego, CA) for Western immunoblotting.

Reagents: Fluorescent probes included Thioflavin T (TFT), JC-1, and Safranin O (MilliporeSigma, St. Louis, MO). Dopamine (DA), $CuCl_2$, H_2O_2 were purchased from ThermoFisher Scientific (Waltham, MA); DOPAL was from Cayman Chemical (An Arbor, MI). Test reagents for mitochondrial protection were purchased either from MilliporeSigma (St. Louis, MO), MedChemExpress (Monmouth Junction, NJ), or European Pharmacopoeia Reference Standards, Chemical Reference Standards (CRS) (see Table 1).

Recombinant Proteins: Human α-synuclein protein (full-length 1-140aa minus NH_2-terminal acetylation) was produced in the UCLA-DOE Protein Expression Technology Center as described previously (Huang et al., 2005) using osmotic shock and ion chromatography. An additional step included size-exclusion chromatography with a Superdex 75 column equilibrated in Tris-buffered saline (TBS). Column purified α-synuclein protein fractions were extensively dialyzed by injection into a low-volume dialysis cassette with the appropriate molecular weight cutoff and exchange buffer in a beaker of water. The α-synuclein solution was removed at a different port than the one used to inject the solution into the cassette and transferred to a low-binding Eppendorf microfuge tube. An equal volume of acetonitrile was added to the protein solution (final solution is 50:50 acetonitrile/water) and flash-frozen in liquid nitrogen and placed in a lyophilizer immediately. Lyophilized α-synuclein powder was stored in aliquots at −80°C until use in fibrillation experiments.

Protein Fibrillation

Recombinant α-synuclein proteins were fibrillated as described (Sarafian et al., 2017). Monomeric protein (40 μM in 50 mM potassium phosphate, pH 7.4) was added to 96-well plates containing 50 mM potassium phosphate buffer (pH 7.4) and 100 mM GdnCl to favor oligomeric formation. A Teflon bead (0.8 μm) was added to each well and solutions were shaken at 300 rpm for 48 hours at 37° C in a Fluoroskan Ascent FL plate reader (ThermoFisher Scientific). Fluorescence was measured in separate wells using 2 μM TFT as probe at 2 hr intervals to monitor aggregation. In some experiments, either dopamine (DA) (200 μM), DOPAL (400 μM) or $CuCl_2$/H_2O_2 (50 μM/100 μM) was added to wells at the onset of fibrillation. Only fibrillated samples lacking TFT were used for subsequent experiments. Following aggregation, some residual free aldehyde was detected in the DOPAL fractions. Accordingly, aldehydes were removed by ZEBA desalting column chromatography (ThermoFisher Scientific) using 0.5 ml spin columns following the manufacturer's protocol. This procedure resulted in a 15% increase in the JC-1 red

fluorescence signal consistent with a direct toxic effect of DOPAL on mitochondria (Kristal et al., 2001). In order to focus exclusively on the effects of α-synuclein proteoforms, only Zeba-purified aggregated forms of α-synuclein were used in toxicity studies. However, since control (untreated) fibrillated α-synuclein failed to elute from Zeba columns, these samples were not subjected to Zeba chromatography.

SDS-PAGE/Immunoblotting

The α-synuclein proteoforms (monomers, aggregates of oligomers and/or fibrils) without Zeba column purification were analyzed by SDS-PAGE using 12% acrylamide gels and a Bio-Rad Mini PROTEAN tetra system as described (Sarafian et al., 2013; Sarafian et al., 2017). Protein concentration was assayed using a Coomassie Blue G-250 Bio-Rad assay with BSA standards. For analysis of higher order fibrillated forms, stacking gels were included in Western immunoblot analyses. Gels were transferred onto PVDF membranes, blocked with 5% nonfat dry milk in Tris-buffered saline plus 0.05% Tween-20 (TBST), and stained with anti-α-synuclein (mouse monoclonal antibody, 1:2,000) followed by HRP-conjugated goat anti-mouse IgG (1:2,500). Membranes were stained with ECL Plus reagent (GE Healthcare) or ECL 2 Western (Thermo Fisher Scientific) and analyzed with a GE 9400 Typhoon Scanner using fluorescence mode.

Transmission Electron Microscopy (TEM)

For negative staining of recombinant proteins, purified α-synuclein monomers and either untreated control-, dopamine-, DOPAL-, or $CuCl_2/H_2O_2$-generated proteoforms (oligomers, fibrils) after 48 hours of fibrillation were deposited on glow-discharged carbon/formvar coated grids and processed for TEM as described (Tsang et al., 2011; Roychaudhuri et al., 2013; Sarafian et al., 2017). Each grid was examined at 60KV on a JEOL 100CX electron microscope. Qualitative observations were made with two separate batches of fibrillated recombinant α-synuclein proteins.

Liquid Chromatography (LC) and Mass Spectrometry (MS)

Top-down MS of intact protein: The same proteins described above for TEM, namely recombinant α-synuclein monomers and either untreated control-, dopamine-, DOPAL-, or $CuCl_2/H_2O_2$-generated proteoforms (oligomers and/or fibrils) were diluted in formic acid to solubilize all proteoforms (3 μl sample plus 30 μl 70% formic acid). Fractions were separated by reverse-phase chromatography with eluent sent to a low-resolution electrospray ionization MS and a fraction collector (LC-MS+) to generate a total ion chromatogram (TIC) as described previously (Sarafian et al., 2013). Intact protein profiles were generated by software deconvolution (MagTran).

Mitochondrial Isolation and Assays

Mitochondrial fractions were isolated from WT mouse (both male and female) forebrain by the MITOISO1 protocol (MilliporeSigma, St. Louis, MO) as described previously (Sarafian et al., 2013). All steps were performed on ice. Following dissection and removal of white matter, the forebrain was split in half along the central commissure and each half minced with a scalpel. The tissue was homogenized by 30 strokes with a hand-held Kontes pellet

pestle motor and conical Teflon pestle in 750 µl in Buffer A (10 mM HEPES, pH 7.5, 200 mM mannitol, 70 mM sucrose,1mM EGTA) plus 2 mg/ml fatty acid-free bovine serum albumin (BSA) in a 1.5 ml microcentrifuge tube. Following centrifugation at 600 × g for 5 min in a refrigerated Eppendorf 5424R desktop centrifuge, the supernatant was removed and the pellet was again homogenized in 500 µl of the same buffer. After a second centrifugation (600 × g, 5 min), the supernatants were combined and centrifuged at 11,000 × g for 10 min. The pellet was resuspended in Buffer A lacking BSA and centrifuged again at 11,000 × g for 10 min. The final pellets (~100 µl) were each resuspended at ~10 mg/ml protein in 120 µl storage buffer (50 mM HEPES, pH7.4, 250 mM sucrose, 1 mM ATP, 0.08 mM ADP, 5 mM succinate, 2 mM K_2HPO_4, 1mM DTT). While the vast majority of experiments used fresh mitochondria prepared on the same day of an experiment, in a few cross-validation experiments, mitochondria were stored at 4°C for an additional 24-48 hours with minor (<25%) loss of membrane potential.

There were two types of mitochondrial assays: membrane potential and oxygen consumption rate (OCR):

Membrane potential:

JC-1: Mitochondria were diluted to 1 mg/ml with storage buffer; α-synuclein proteoforms (monomers, aggregates) were diluted to 10 µM with 10 mM Tris pH 7.4. Aliquots (40 µl each) of mitochondria were preincubated with α-synuclein protein samples (5 µl) for 15 minutes at room temperature. Subsequently 5 µl each was added to 45 µl of JC-1 assay buffer containing 1µg/µl JC-1 in quadruplicate wells of a 96-well plate. Red (E_x=530, E_m=590) and green (E_x=485, E_m=538) fluorescence was measured at 2, 15, and 30 minute in a clear flat-well 96-well plate (Costar) using a Fluoroskan Ascent FL plate reader. Red fluorescence at 30 minutes was used as a measure of mitochondrial membrane potential. N.B. Some JC-1 mitochondrial experiments were excluded when control values for membrane potential differed by > 50% from the mean of all experiments. The ability of test reagents to protect against DOS toxicity utilized the same JC-1 protocol except that the test reagents were added to the mitochondria 15 minutes prior to exposure to DOS. For some experiments, excess DOS was washed away to remove background fluorescence. Following incubation with DOS for 30 minutes at 30°C, mitochondria were washed free of unbound DOS by centrifugation at 8,000 × *g* for 1 min. The pellet was re-suspended in 200 µl storage buffer and centrifugation was repeated. The resulting pellet was re-suspended in 50 µl storage buffer and membrane potential was assayed with JC-1 as above.

Safranin O: The histological agent Safranin O (Figueira et al., 2012; Krumschnabel et al., 2014) was used as an alternative fluorescent reagent to cross-validate alterations in mitochondrial membrane potential. Following 30 minute incubation with DOS at 30°C, mitochondria were washed free of external DOS as described above and added to wells containing 50 µl assay buffer and 5 µM Safranin O. Red fluorescence was measured at 1 and 20 minutes in a plate reader. In this assay, healthy control mitochondria quench Safranin O red fluorescence as a function of membrane potential, while injured mitochondria display diminished quenching.

OCR: A Seahorse (Agilent) XF96 Analyzer was used to determine the OCR in isolated mitochondria treated with α-synuclein proteoforms (monomers, aggregates) in the UCLA DGSOM Metabolism Core as described (Rogers et al., 2011; Mahdaviani et al., 2017). DOS (DOS 10= 6.7 μM) and other control α-synuclein proteoforms (monomers, untreated fibrils, dopamine-derived aggregates) were pre-incubated with isolated mouse forebrain mitochondria (0.7 mg/ml) in storage buffer for 60 minutes at 30oC in 0.5 ml Eppendorf tubes and quenched on ice until processing with the Seahorse XF96Analyzer.

The injection ports of the XF96 Assay Cartridge were loaded with compounds to be injected during the assay. The isolated mitochondrial conditions included in this order injections of: ADP (4 μM); the ATP Synthase inhibitor, oligomycin (3 μM); the chemical uncoupler, FCCP (4 μM); and the Complex I and Complex III inhibitors, rotenone and antimycin A (4 μM each), to halt all mitochondrial respiration. These conditions allow for the determination of State 2, 3 and 4o respiration as well as uncoupled and non-mitochondrial respiration and the respiratory control ratio (RCR). N.B. Only healthy mitochondria that exhibited substantially elevated State 3 values above State 2 baseline values were used in OCR experiments. Once the ports were loaded, the cartridge was placed in the XF96 Extracellular Flux Analyzer for calibration. During the 30 minute cartridge calibration period, isolated mitochondria (with and without α-synuclein proteoforms) were loaded into the XF96 microplate on ice with 15 μl of 10X substrate solution (pyruvate and malate (Complex I) or succinate and rotenone (Complex II). Final concentrations were 5 mM for pyruvate, malate, and succinate and 2 μM for rotenone. A total of *6 μg* of protein was loaded per well into a XF96 cell culture microplate for Complex-I driven respiration and *4 μg* per well was loaded for Complex II-driven respiration. The XF96 plate was then centrifuged at 3,400 rpm for 10 minutes to adhere the mitochondria to the plate. After centrifugation, the total volume of the well was adjusted to 150 μl with ice cold mitochondrial assay solution (MAS: 70 mM sucrose, 220 mM mannitol, 5 mM KH_2PO_4, 5 mM $MgCl_2$, 2mM HEPES, 1 mM EGTA, 0.1 % BSA fatty acid-free, pH 7.2 adjusted with 1 M KOH). The loaded plates were incubated at 37°C in a non-CO_2 incubator for approximately 8 minutes before loading into the XF96 instrument once the calibration was completed. Final measurements consisted of a series of standardized injections, mixes and measurements for each compound (ADP, oligomycin, FCCP, rotenone/antimycin). Graphs/Histograms for OCR values (picomoles/min/μg protein) were generated with Agilent software (Wave Desktop)(UCLA DGSOM Metabolism Core Facility).

Statistical Analysis

Student's *t*-tests were used for two group comparisons. One Way ANOVAs were used for comparisons among multiple groups followed by the appropriate post-hoc *t*-tests for pairwise comparisons (Sigma Plot 10/11, RRID: SCR_003210) (Watson et al., 2009; Sarafian et al., 2013; Sarafian et al. 2017).

RESULTS

Enhanced Oligomerization of α-Synuclein by Incubation with DOPAL

Thioflavin T (TFT) Time Course of Fibrillation—A previous study from this lab (Sarafian et al., 2017) showed that recombinant human α-synuclein was efficiently aggregated by shaking for 48 hours in a 96-well plate format to form amyloid fibrils in the presence of either 100 mM NaCl or 100 mM GdnCl. Notably fibrillation was attenuated with GdnCl as measured by TFT fluorescence. Use of oligomer-selective fluorescent probes (DCVJ, ANS) (Bolognesi et al., 2010; Paslawski et al., 2014) and electron microscopy revealed that GdnCl favored the production of oligomeric forms of α-synuclein along with elongated fibers. In light of this observation, GdnCl was used to preferentially select for oligomer formation in all fibrillation studies described here.

Based on previous reports (Post et al., 2018), both dopamine and its oxidative deaminated metabolite, DOPAL, also enhanced the production of stable oligomeric forms of α-synuclein. To further promote this process, recombinant α-synuclein protein was fibrillated in the presence of GdnCl together with either dopamine, DOPAL, or $CuCl_2/H_2O_2$ as a control for oxidation conditions (Paik et al., 2000; Follmer et al., 2015; Mor and Ischiropoulos, 2018; Mor et al., 2019). As shown in Figure 1A, aggregation of untreated α-synuclein (control panel, bottom left) followed a normal time course of TFT fluorescence with a lag, exponential and stationary phase for amyloid structures enriched in β-sheet. Inclusion of both dopamine and $CuCl_2/H_2O_2$ produced much different TFT profiles in which the fluorescence amplitudes of all phases were reduced (TFT probe, lower panels). Time courses without the TFT probe (top panels) were flat for all treatments, except DOPAL, which resulted in an accelerated increase in green fluorescence followed by a rapid decline. This increase did not occur without the presence of α-synuclein (see Fig. 1B) and was likely related to pyrrole dicatechol adducts linked to lysines in α-synuclein aggregates (Coelho-Cerqueira et al., 2014; Follmer et al., 2015; Werner-Allen et al., 2016)(also see Fig. 4).

SDS-PAGE/Immunoblotting of Aggregated α-Synuclein—The results from TFT time course studies strongly suggested that all three treatments (dopamine, DOPAL, $CuCl_2/H_2O_2$) selected for smaller α-synuclein structures, possibly oligomeric in nature. This proposal was initially borne out by resolution of α-synuclein proteoform bands on Western immunoblots (Fig. 2A). When compared to purified recombinant α-synuclein (far left lane), a smear of likely oligomeric bands ≥ 37 kDa was detected in fibrillated α-synuclein mainly in the presence of DOPAL but to a lesser extent in dopamine- and $CuCl_2/H_2O_2$ -treated samples and much less so in untreated, control samples. Larger species detected in the stacking gel (>250 kDa) are likely a combination of larger oligomeric/protofibrillary structures as well as mature fibrils found in the wells. The observed increase in α-synuclein intrinsic fluorescence caused by DOPAL conjugation (Fig. 1) raised the possibility that the prominent increase in higher molecular weight banding on Western gels analyzed by ECL fluorescence detection was not due to an increase in protein. To investigate this in more detail, the same protein samples were resolved by SDS-PAGE alone and stained directly with Coomassie brilliant blue R250 (Fig. 2B). Staining revealed that numerous higher molecular weight bands were produced that corresponded to similar Western bands present

in the DOPAL lane. Other treatments including dopamine produced far less oligomeric bands. The DOPAL banding pattern was stable for samples stored at −80°C for over one year and after several freeze-thaw cycles.

Transmission Electron microscopy (TEM) of Aggregated α-Synuclein—As an additional examination of potential DOPAL-generated proteoforms of α-synuclein, identical samples previously processed for protein gels were examined by TEM. DOPAL-derived aggregates were revealed predominantly as large chains of oligomeric-like structures (Fig. 3C, far right, top panel). Thus, consistent with previous reports (Follmer et al., 2015; Werner-Allen et al., 2016;Werner-Allen et al., 2017; Werner-Allen et al., 2018), DOPAL preferentially selected for oligomeric forms of α-synuclein. In contrast, recombinant protein alone was mainly monomeric (Fig. 3A), while untreated fibrillated protein appeared mainly as long mature fibers and some oligomers (Fig. 3B). Both dopamine- and $CuCl_2/H_2O_2$-derived aggregates (Fig. 3D, E, bottom panels) were a combination of fibrils and likely oligomers. Quite striking and unique to the dopamine aggregates, beads of oligomeric-like structures decorated many of the fibrils.

Enhanced Covalent Modifications of DOPAL-Aggregated α-Synuclein Revealed by Top-Down Mass Spectrometry (MS)

Previous reports detected multiple forms of DOPAL-derived covalent modifications of lysines (catechols, quinones, cross-linked adducts) and methionine oxidations of both α-synuclein monomers and oligomers that inhibited amyloid fibril formation (Follmer et al., 2015; Werner-Allen et al., 2016; Plotegher et al., 2017; Werner-Allen et al., 2017; Werner-Allen et al., 2018). These studies employed bottom-up MS analyses of partial tryptic peptides, so not all of the amino acid residues in the intact full-length α-synuclein proteoforms were sampled.

To complement previous bottom-up approaches, a top-down MS analysis was performed on untreated control-, dopamine-, DOPAL-, or $CuCl_2/H_2O_2$-generated proteoforms (oligomers and/or fibrils) of intact, full-length α-synuclein. Samples were rigorously solubilized with an excess amount of formic acid to reduce all forms to monomeric size retaining potential covalent modifications. As shown in Figure 4, mostly unmodified monomers (mass, 14458.4) were detected in control samples of untreated fibrillated α-synuclein (Fig. 4A); a similar profile was observed for untreated monomers (not shown). However, many additional species of higher molecular weight were detected in DOPAL-treated α-synuclein (Fig. 4C). For example, there are four prominent peaks at masses 14475 (+16), 14491 (+32), 14507 (+48), 14523 (+64), likely due to oxidation of the four methionines found in full-length α-synuclein but with little or no unmodified monomer detected (Glaser et al., 2005; Sarafian et al., 2013; Carmo-Goncalves et al., 2018). Additional multiple heavier peaks approximating the expected masses of quinones and catechol modifications of lysines were also detected in the DOPAL-derived aggregates. In support of this proposal, both Michael Additions and Schiff base modifications of lysine residues in α-synuclein were detected by bottom-up MS analyses of tryptic peptides of DOPAL-derived aggregates (data not shown) (also see Follmer et al., 2015).

In contrast, the unmodified α-synuclein monomer was clearly detected in dopamine aggregates (Fig. 4B), while fewer heavier peaks including methionine oxidation were detected relative to the DOPAL aggregates. In this regard, dopamine is not known to covalently modify α-synuclein (Conway et al., 2001; Mor and Ischiropoulos, 2018). As expected, $CuCl_2/H_2O_2$ aggregates (Fig. 4D) were fully oxidized with little or no unmodified monomer. Thus, the top-down MS studies were consistent with the proposal that DOPAL-mediated methionine oxidations together with covalent modifications of lysines in the full length α-synuclein protein preferentially promote its oligomer formation at the expense of amyloid fibril formation.

DOS Inhibits Mitochondrial Functions

Decreased Respiratory Control Ratio for Oxygen Consumption—Having derived a stable population of DOPAL-oligomerized α-synuclein (now referred to as DOS) likely related to PD neuropathology, DOS' potential toxic effect on mouse brain mitochondria was analyzed *in vitro* by multiple functional assays. The Seahorse XF96 Analyzer technology was utilized to measure the OCR of freshly isolated mouse forebrain mitochondria pre-incubated with DOS for 60 minutes at 30°C.

As shown in Figure 5A (one representative experiment), DOS appeared to produce a concentration-dependent decrease in State 3 respiration using pyruvate plus malate (complex I pathway) as substrates (ADP added), with no effect on State 2 oxygen consumption. The highest levels of DOS (DOS 10 = 6.7 μM) reduced the State 3 OCR by ~50%. The State 4 respiration rate (FCCP uncoupled) was similarly inhibited suggesting that the electron transport chain was impaired. Notably, analysis of all experiments (N=4)(Fig. 5B, left panel) showed that the OCR (State 3-State 2) was significantly different for the pyruvate plus malate complex I pathway at all ranges of DOS (DOS 2, 5, 10/($p<0.01$, $p<0.01$, $p<0.001$ respectively, Bonferroni post-hoc tests, One Way ANOVA). Moreover, the critical Respiratory Control Ratio (RCR, ratio of State 3/State 2) (Brand and Nicholls, 2011) for the pyruvate plus malate pathway was significantly reduced at the DOS 10 concentration (Fig. 5B, right panel, $p<0.05$, Bonferroni post-hoc test, One Way ANOVA). Using succinate as substrate in the presence of rotenone (selecting for entry at the complex II pathway), significant inhibition was not observed (Fig. 5C) ($p=0.06$, not significant, One Way ANOVA), suggesting that the complex I pathway (pyruvate plus malate entrance point) was more sensitive to DOS. Recombinant protein alone (monomeric) and untreated, fibrillated α-synuclein had little to no effect in this assay (data not shown). Dopamine-derived α-synuclein aggregates also appeared to produce a reduction in pyruvate/malate fueled State 3 respiration, although to a lesser degree than DOS at similar α-synuclein equivalents (not shown).

Decreased Membrane Potential—In addition to measuring OCR, mitochondrial membrane potential was measured using JC-1 red fluorescence to evaluate the effect of short-term (15-60 minute) exposure to α-synuclein aggregates (Fig. 6). As expected, FCCP significantly decreased the membrane potential but recombinant monomeric α-synuclein protein did not (Fig. 6A, left panel)(FCCP vs control buffer alone, $p<0.001$, Bonferroni post-hoc test, One Way ANOVA). Untreated aggregated (48 hour) α-synuclein (Fig. 6A, right

panel) had little or no effect on JC-1 fluorescence, in contrast to previous results detecting membrane potential inhibition in overexpressing mice (Sarafian et al., 2013). $CuCl_2/H_2O_2$ oxidized α-synuclein also had no effect. However, comparing similar α-synuclein equivalents, both dopamine (DA)-aggregates and DOPAL aggregates (aka DOS) lowered the JC-1 fluorescence when compared to untreated aggregated controls (DA ± Zeba column, $p<0.01$, Bonferroni post-hoc test; DOPAL ± Zeba column $p<0.001$, Bonferroni post-hoc test, One Way ANOVA). Thus DOS caused considerably more inhibition than dopamine aggregates.

Surprisingly, DOS alone had the ability to partially lower background JC-1 red fluorescence in the absence of mitochondria. In order to avoid background fluorescent effects, additional control experiments were performed in which DOS (DOS 5, 10) was pre-incubated with mitochondria followed by removal of free DOS by centrifugation and extensive washing with buffer. DOS removal was confirmed by exposing supernatant to solutions of JC-1 (not shown). Importantly pretreated/washed mitochondria displayed lower JC-1 red fluorescence, reaffirming diminished membrane potential in response to DOS (Fig. 6B)(DOS 5, $p<0.05$, DOS 10; $p<0.01$, Paired-*t* test). The degree of inhibition observed in the pre-incubation protocol was concentration-dependent and temperature-sensitive.

To further corroborate the effect of DOS on mitochondrial membrane potential, an alternative fluorescent probe was tested. Safranin O is a histochemical staining agent which can be used for cellular and cell-free mitochondrial assays (Figueira et al., 2012; Krumschnabel et al., 2014). A high negative membrane potential promotes uptake of Safranin O, which is accompanied by a quenching of red fluorescence. Injured mitochondria produce a lower degree of quenching. Using this assay (Fig. 6C), DOS 5 was found to reduce the quenching of 1 μM Safranin O ($p<0.01$, Paired ***t***-test). Note: measurements were taken rapidly after addition of mitochondria to Safranin O as the quenching effect diminishes over time.

Screening for Mitochondrial Protective Agents

A customized targeted library of 39 commercially available compounds was tested for utility to protect against DOS-induced mitochondrial injury (Table 1). Compounds reported to have mitochondrial- or PD-related effects were screened at concentrations of 50 and 250 μM using the JC-1 assay. Drugs were initially tested once in a limited throughput approach by pre-incubation for 15 min at room temperature prior to exposure to DOS in order to allow access to mitochondrial compartments. The majority of these compounds (58%) had no effect on DOS inhibition (Note: threshold was > 10 % protection of membrane potential to be scored as a positive result). Included in the group of negative responses for protection were anti-oxidants: N-acetylcysteine, ascorbic acid, butylated hydroxyanisole and deferoxamine. The mitochondrial permeability transition blocker, cyclosporin A (Lemasters, 1999) also failed to provide significant protection. Several (as many as 11) compounds had strong inhibitory effects on their own at the concentrations tested.

Four unrelated compounds reversed the decrease in JC-1 red fluorescence caused by DOS and were scored as positives. In follow up experiments, dose response curves for membrane potential were generated for each compound (Fig. 7A-D), which were significantly higher

than untreated DOS controls alone (Coenzyme Q10, $p<0.001$; Fenofibrate, $p<0.001$; Ginsenoside Re, $p<0.001$; Mitochondrial division inhibitor-1, $p<0.001$, One Way ANOVA). Over a broad concentration range (25-250 μM), Coenzyme Q10 (CoQ) (Fig. 7A) completely restored DOS-mediated decrease in mitochondrial membrane potential ($p<0.001$, Fisher LSD post-hoc tests). Ginsenoside Re (Fig. 7C) partially restored JC-1 red fluorescence at 50 and 100 μM and fully at 250 μM ($p<0.001$, Fisher LSD post-hoc tests). Both fenofibrate and mitochondrial division inhibitor-1 (Mdiv-1) (Fig. 7B, D) produced peak protection at 100 μM ($p<0.001$, Fisher LSD post-hoc tests) and their effects greatly diminished at 250 μM suggesting inhibitory effects at higher concentrations. Only one compound, Mdiv-1, independently increased the background red fluorescence of JC-1. None of the protective compounds tested significantly altered the DOS oligomeric structures (large or small) based on Western blotting (Fig. 7E, top panel). The same was true for the majority of the other compounds in the customized library, although lycopene and mitoquinone mesylate appeared to reduce the sharpness of monomeric and small oligomeric bands (Fig. 7E, bottom panel).

DISCUSSION

Early studies of post-mortem brain tissue from PD patients identified the loss of dopaminergic neurons particularly in the substantia nigra pars compacta (Forno, 1996; Youdim and Riederer, 1997; Dauer and Przedborski, 2003). In an effort to understand the selective vulnerability of these cells, much effort has focused on the toxicity of dopamine whose oxidation can generate quinones and reactive oxygen species (ROS) causing oxidative stress and cellular damage (Mor and Ischiropoulos, 2018; Mor et al. 2019). Dopamine, if not recycled by synaptic vesicularization, is degraded by monoamine oxidases A and B to DOPAL (3,4-dihydroxyphenylacetaldehyde) and then by aldehyde dehydrogenase to form DOPAC. However, DOPAL is more neurotoxic than dopamine due to its reactive aldehyde (Kristal et al., 2001; Li et al., 2001; Burke et al., 2003; Galvin, 2006; Burke et al., 2008). Levels of DOPAL were found to be higher in brain tissue from PD patients relative to non-PD brain tissue (Goldstein et al., 2011; Goldstein et al., 2013). Together these findings have led to the “catecholaldehyde hypothesis” (Burke et al., 2003; Rees et al., 2009; Panneton et al., 2010; Anderson et al., 2011; Goldstein et al., 2012; Casida et al., 2014) as the basis of PD. Support for the hypothesis has come from studies demonstrating that some pesticides linked to PD in humans and animal models cause inhibition of the alcohol dehydrogenase enzyme with resultant accumulation of DOPAL (Staub et al., 1999; Fitzmaurice et al., 2013).

While both dopamine and $CuCl_2/H_2O_2$ suppress fibril formation, the resulting oligomers appeared to have relatively low mitochondrial toxicity based on OCR and membrane potential measurements (also see Paik et al., 2000; Zhou et al., 2010). Dopamine oxidation has been shown to promote the formation of toxic α-synuclein oligomers in a way that is non-covalent, reversible and targeted mainly to conformational changes in the carboxyl terminus (Mazzulli et al., 2006; Mor et al., 2019). Exposure to $CuCl_2/H_2O_2$ promotes oligomer formation by oxidizing α-synuclein methionines and forming dityrosine cross-links (Kowalik-Jankowska et al., 2008; Al-Hilaly et al., 2016). Aggregation with DOPAL not only produces ROS and α-synuclein oxidation at methionines and lysines, but also multiple covalent modifications including dicatechol pyrrole cross linking at an abundant number of

lysines based on bottom-up MS studies of tryptic peptides. Importantly, the top-down MS analyses shown here represent the first demonstration of covalent modifications of aggregates of the intact α-synuclein protein by DOPAL and were consistent with previous bottom-up studies, namely methionine oxidation and likely lysine modifications. (Werner-Allen et al., 2016). In our hands, the DOS fibrillation reactions were also accompanied by a rapid enhancement of intrinsic fluorescence, which peaked at around 12 hours and declined ~50% thereafter. This fluorescence pattern is not evident with DOPAL alone and is not altered by the inclusion of TFT indicating that amyloid fibril formation may have diminished. Intrinsic DOS fluorescence (both red and green) was not high enough to interfere with fluorescent mitochondrial assays used here.

In the present study, isolated brain mitochondria were used in order to allow direct exposure of DOS and other α-synuclein aggregated proteoforms to the organelle without having to traverse the cell plasma membrane. This approach permitted the use of lower concentrations of DOS to produce mitochondrial effects comparable to cell culture models. Importantly, this method also mimics the cytosolic environment in which both DOPAL and α-synuclein aggregates are primarily generated in the neuronal cytoplasm, where they would interact to form toxic oligomers and have direct access to mitochondria. Numerous reports have shown that aggregated forms of α-synuclein can penetrate membranous structures and gain access to intracellular compartments (Camilleri et al., 2013; Lorenzen et al., 2014; Mahul-Mellier et al., 2015; Pacheco et al., 2015; Peelaerts et al., 2015). For example, DOPAL-derived oligomers can permeabilize membranes and impair synaptic vesicle function (Plotegher et al., 2017). It is also noteworthy that DOPAL-modified oligomers display greater stability, while modified monomers showed weaker interactions with lipid membranes (Follmer et al., 2015). Thus, the use of this preparation should reduce the problem of dynamic instability and heterogeneity of α-synuclein oligomers often encountered with other protocols.

Using two different fluorescent probes, DOS was shown to directly impair mitochondrial membrane potential. To our knowledge, the direct toxic effect of DOS on mitochondria has not been previously reported. DOS impairment was enhanced relative to either dopamine- or $CuCl_2/H_2O_2$-treated samples, suggesting that catechols, quinones, and cross-linked adducts at lysines were key modifications. Similar toxicity was observed when measuring mitochondrial respiration, particularly when driven by pyruvate plus malate. The latter results strongly implicate mitochondrial complex I as a target for DOS in mitochondrial toxicity, consistent with numerous reports of a major role for complex I in PD (Schapira et al., 1990). Since DOPAL alone has also been shown to inhibit mitochondria (Kristal et al., 2001), it is possible that there is a two-hit mechanism of toxicity operational in PD, in which both DOPAL and DOS work together to inhibit mitochondria. However, unlike DOPAL which is removed metabolically via aldehyde dehydrogenases, DOS oligomers contain DOPAL-covalently conjugated as adducts to one or more amino acids, principally lysines. Since covalent modifications are for the most part irreversible save by enzyme activity, the half-life of DOS may be much longer than most other oligomeric structures and thus more apt to accumulate and become toxic.

Identifying small molecules that block DOS-induced mitochondrial injury could suggest mechanisms of toxic action as well as identify possible pharmacological therapeutic agents

to delay or prevent PD neuropathology. In this study, an initial trial was conducted with a small number of known, commercially available compounds to demonstrate the utility of DOS in screening for potential drug rescue of PD-related mitochondrial deficits. Since oxidative stress is a likely contributing factor in PD pathogenesis (Mor et al., 2019) and various α-synuclein oligomer preparations have been shown to cause oxidative injury (Parihar et al., 2008; Gallegos et al., 2015; Ludtmann et al., 2018), a variety of anti-oxidants were screened as potential DOS blockers. However, most of the classic antioxidants tested in this study, including ascorbic acid, butylated hydroxyanisole, deferoxamine, and N-acetylcystine did not protect against DOS-induced mitochondrial injury. This suggested that oxidative stress did not mediate the observed injury. However, four unrelated compounds from a list of 39 or more were shown to protect against DOS-induced mitochondrial injury. These included: fenofibrate, ginsenoside Re, CoQ, and Mdiv-1. A brief discussion is provided below for each compound's potential actions.

Fenofibrate has been reported to both impair (Brunmair et al., 2004) and protect mitochondria (Hong et al., 2016). While it acts primarily to activate PPAR α to induce antioxidant and anti-inflammatory properties, in mitochondria it may interact directly with complex I of the electron transport chain. Such an interaction, while likely to inhibit complex I activity, may serve to protect against the effects of DOS.

Ginsenoside Re and other ginsenosides have anti-oxidant effects directly and also through the Nrf-2 antioxidant response element as with fenofibrate (Gonzalez-Burgos et al., 2017; Tran et al., 2017). Similarly it appears to have the ability to protect complex I in mitochondria, since neuronal protection against rotenone and MPTP have been demonstrated (Leung et al., 2007; Liu et al., 2015). The rapid protective effects of fenofibrate and ginsenoside against DOS in our isolated mitochondria preparation, which should not contain whole cells or intact nuclei, suggests that a direct interaction with complex I mediates their effect. Notably, ginsenoside Rb1, which has been reported to disaggregate α-synuclein oligomers and protect both BE(2)-M17 neuroblastoma cells (Ardah et al., 2015) and dopaminergic cells in an MPTP PD mouse model (Zhang et al., 2018), failed to protect mitochondria from effects of DOS or to disaggregate DOS oligomers (data not shown).

Mdiv-1 inhibits the GTPase activity of the mitochondrial fission-inducing protein Drp-1 (Smith and Gallo, 2017; Manczak et al., 2019). This inhibition of mitochondrial fission results in neuronal protection in experimental models of Alzheimer's disease, ischemia, and epilepsy (Kim et al., 2016; Bido et al., 2017; Kim et al., 2017). However, a recent report indicates that Mdiv-1 exerts a DRP-1-independent effect on mitochondria by inhibiting complex I and reducing mitochondrial ROS production (Bordt et al., 2017). Thus it was surprising it had a blocking, rescue effect relative to DOS exposure, suggesting a possible occlusion mechanism.

CoQ, also known as ubiquinol, is a highly lipophilic compound with a redox-active benzoquinone ring attached to a hydrophobic chain of 10 isoprenoid units (Nakajima et al., 2008, Villalba et al., 2010; Bergamini et al., 2012; Garrido-Maraver et al., 2014). The benzoquinone ring provides antioxidant and free radical scavenging activity. CoQ also has

an ability to alter the expression of numerous genes affecting metabolism, cell signaling, and inflammation. Its primary function is to serve as a co-factor in the mitochondrial electron transport chain where it shuttles electrons from both complex I and complex II to complex III. In this role, CoQ has the ability to directly interact with complex I and improve its function in the electron transport chain which drives the mitochondrial membrane potential and ATP synthesis. Thus, the ability to interact with complex I seems to be the common feature among the agents reducing the inhibitory effect of DOS on mitochondrial membrane potential.

In conclusion, we have used the dopamine metabolite, DOPAL, and GdnCl to enhance oligomerization of recombinant α-synuclein by an agitation protocol conducted for 48 hr at 37°C. Compared with control-, dopamine-, and $CuCl_2/H_2O_2$-fibrillated α-synuclein, DOPAL appeared to produce the highest amount of oligomerized α-synuclein when examined by Western immunoblotting and TEM. When added to isolated mouse brain mitochondria, DOS displayed the highest toxicity in Seahorse-based respiration and mitochondrial membrane potential assays. We used a customized chemical library to screen for protection against DOS-induced loss of mitochondrial membrane potential and identified at least four dissimilar compounds with protective capability. Overall, results suggest that complex I may be the primary target of DOS-induced mitochondrial injury. Future plans include the development of a cellular model for DOS-induced mitochondrial injury and the use of high-throughput screening for protective agents.

ACKNOWLEDGEMENTS

Special thanks to the Cepeda-Levine lab especially Sandra Holley and Joshua Barry for providing mice and general input on the manuscript. Elissa Donzis deserves additional thanks for expertise on artwork, illustrations, and statistical analyses. Multiple UCLA Cores also deserve thanks for their critical services including Marianne Cilluffo and Chunni Zhu in the Brain Research Institute's Electron Microscopy Core, Mark Arbing in the UCLA-DOE Protein Expression Technology Center, and Linsey Stiles in the UCLA DGSOM Metabolism Core. Dr. Robert Damoiseaux and Bobby Tofig in the Molecular Screening Shared Resource also provided invaluable advice for small molecule experiments. The authors thank Raymond Guan and Jenna Smith for technical assistance and manuscript preparation.

FUNDING: Julian Whitelegge was supported by the UCSD/UCLA Diabetes Research Center (P30 DK063491). UCLA-DOE Protein Expression Technology Center was supported by the U.S. Department of Energy, Office of Biological and Environmental Research (BER) program under Award Number DE-FC02-02ER63421.

REFERENCES

Al-Hilaly YK, Biasetti L, Blakeman BJ, Pollack SJ, Zibaee S, Abdul-Sada A, Thorpe JR, Xue WF and Serpell LC (2016). The involvement of dityrosine crosslinking in alpha-synuclein assembly and deposition in Lewy Bodies in Parkinson's disease. Sci Rep 6, 39171 10.1038/srep39171 [PubMed: 27982082]

Ammal Kaidery N and Thomas B (2018). Current perspective of mitochondrial biology in Parkinson's disease. Neurochem Int 117, 91–113. 10.1016/j.neuint.2018.03.001 [PubMed: 29550604]

Anderson DG, Mariappan SV, Buettner GR and Doorn JA (2011). Oxidation of 3,4-dihydroxyphenylacetaldehyde, a toxic dopaminergic metabolite, to a semiquinone radical and an ortho-quinone. J Biol Chem 286(30), 26978–26986. 10.1074/jbc.M111.249532 [PubMed: 21642436]

Ardah MT, Paleologou KE, Lv G, Menon SA, Abul Khair SB, Lu JH, Safieh-Garabedian B, Al-Hayani AA, Eliezer D, Li M and El-Agnaf OM (2015). Ginsenoside Rb1 inhibits fibrillation and toxicity of

alpha-synuclein and disaggregates preformed fibrils. Neurobiol Dis 74, 89–101. 10.1016/j.nbd.2014.11.007 [PubMed: 25449909]

Bergamini C, Moruzzi N, Sblendido A, Lenaz G and Fato R (2012). A water soluble CoQ10 formulation improves intracellular distribution and promotes mitochondrial respiration in cultured cells. PLoS One 7(3), e33712 10.1371/journal.pone.0033712 [PubMed: 22432044]

Bido S, Soria FN, Fan RZ, Bezard E and Tieu K (2017). Mitochondrial division inhibitor-1 is neuroprotective in the A53T-alpha-synuclein rat model of Parkinson's disease. Sci Rep 7(1), 7495 10.1038/s41598-017-07181-0 [PubMed: 28790323]

Bolognesi B, Kumita JR, Barros TP, Esbjorner EK, Luheshi LM, Crowther DC, Wilson MR, Dobson CM, Favrin G and Yerbury JJ (2010). ANS binding reveals common features of cytotoxic amyloid species. ACS Chem Biol 5(8), 735–740. 10.1021/cb1001203 [PubMed: 20550130]

Bordt EA, Clerc P, Roelofs BA, Saladino AJ, Tretter L, Adam-Vizi V, Cherok E, Khalil A, Yadava N, Ge SX, Francis TC, Kennedy NW, Picton LK, Kumar T, Uppuluri S, Miller AM, Itoh K, Karbowski M, Sesaki H, Hill RB and Polster BM (2017). The Putative Drp1 Inhibitor mdivi-1 Is a Reversible Mitochondrial Complex I Inhibitor that Modulates Reactive Oxygen Species. Dev Cell 40(6), 583–594 e586. 10.1016/j.devcel.2017.02.020 [PubMed: 28350990]

Bose A and Beal MF (2016). Mitochondrial dysfunction in Parkinson's disease. J Neurochem 139 Suppl 1, 216–231. 10.1111/jnc.13731 [PubMed: 27546335]

Brand MD and Nicholls DG (2011). Assessing mitochondrial dysfunction in cells. Biochem J 435(2), 297–312. 10.1042/BJ20110162 [PubMed: 21726199]

Brunmair B, Lest A, Staniek K, Gras F, Scharf N, Roden M, Nohl H, Waldhausl W and Furnsinn C (2004). Fenofibrate impairs rat mitochondrial function by inhibition of respiratory complex I. J Pharmacol Exp Ther 311(1), 109–114. 10.1124/jpet.104.068312 [PubMed: 15166256]

Burke WJ, Kumar VB, Pandey N, Panneton WM, Gan Q, Franko MW, O'Dell M, Li SW, Pan Y, Chung HD and Galvin JE (2008). Aggregation of alpha-synuclein by DOPAL, the monoamine oxidase metabolite of dopamine. Acta Neuropathol 115(2), 193–203. 10.1007/s00401-007-0303-9 [PubMed: 17965867]

Burke WJ, Li SW, Williams EA, Nonneman R and Zahm DS (2003). 3,4-Dihydroxyphenylacetaldehyde is the toxic dopamine metabolite in vivo: implications for Parkinson's disease pathogenesis. Brain Res 989(2), 205–213. [PubMed: 14556942]

Camilleri A, Zarb C, Caruana M, Ostermeier U, Ghio S, Hogen T, Schmidt F, Giese A and Vassallo N (2013). Mitochondrial membrane permeabilisation by amyloid aggregates and protection by polyphenols. Biochim Biophys Acta 1828(11), 2532–2543. 10.1016/j.bbamem.2013.06.026 [PubMed: 23817009]

Carmo-Goncalves P, do Nascimento LA, Cortines JR, Eliezer D, Romao L and Follmer C (2018). Exploring the role of methionine residues on the oligomerization and neurotoxic properties of DOPAL-modified alpha-synuclein. Biochem Biophys Res Commun 505(1), 295–301. 10.1016/j.bbrc.2018.09.111 [PubMed: 30249394]

Casida JE, Ford B, Jinsmaa Y, Sullivan P, Cooney A and Goldstein DS (2014). Benomyl, aldehyde dehydrogenase, DOPAL, and the catecholaldehyde hypothesis for the pathogenesis of Parkinson's disease. Chem Res Toxicol 27(8), 1359–1361. 10.1021/tx5002223 [PubMed: 25045800]

Coelho-Cerqueira E, Pinheiro AS and Follmer C (2014). Pitfalls associated with the use of Thioflavin-T to monitor anti-fibrillogenic activity. Bioorg Med Chem Lett 24(14), 3194–3198. 10.1016/j.bmcl.2014.04.072 [PubMed: 24835632]

Conway KA, Rochet JC, Bieganski RM and Lansbury PT Jr. (2001). Kinetic stabilization of the alpha-synuclein protofibril by a dopamine-alpha-synuclein adduct. Science 294(5545), 1346–1349. 10.1126/science.1063522 [PubMed: 11701929]

Cremades N, Chen SW and Dobson CM (2017). Structural Characteristics of alpha-Synuclein Oligomers. Int Rev Cell Mol Biol 329, 79–143. 10.1016/bs.ircmb.2016.08.010 [PubMed: 28109332]

Dauer W and Przedborski S (2003). Parkinson's disease: mechanisms and models. Neuron 39(6), 889–909. [PubMed: 12971891]

Devi L, Raghavendran V, Prabhu BM, Avadhani NG and Anandatheerthavarada HK (2008). Mitochondrial import and accumulation of alpha-synuclein impair complex I in human

dopaminergic neuronal cultures and Parkinson disease brain. J Biol Chem 283(14), 9089–9100. [PubMed: 18245082]

Di Maio R, Barrett PJ, Hoffman EK, Barrett CW, Zharikov A, Borah A, Hu X, McCoy J, Chu CT, Burton EA, Hastings TG and Greenamyre JT (2016). alpha-Synuclein binds to TOM20 and inhibits mitochondrial protein import in Parkinson's disease. Sci Transl Med 8(342), 342ra378 10.1126/scitranslmed.aaf3634

Figueira TR, Melo DR, Vercesi AE and Castilho RF (2012). Safranine as a fluorescent probe for the evaluation of mitochondrial membrane potential in isolated organelles and permeabilized cells. Methods Mol Biol 810, 103–117. 10.1007/978-1-61779-382-0_7 [PubMed: 22057563]

Fischer AF and Matera KM (2015). Stabilization of Alpha-Synuclein Oligomers In Vitro by the Neurotransmitters, Dopamine and Norepinephrine: The Effect of Oxidized Catecholamines. Neurochem Res 40(7), 1341–1349. 10.1007/s11064-015-1597-y [PubMed: 25956992]

Fitzmaurice AG, Rhodes SL, Lulla A, Murphy NP, Lam HA, O'Donnell KC, Barnhill L, Casida JE, Cockburn M, Sagasti A, Stahl MC, Maidment NT, Ritz B and Bronstein JM (2013). Aldehyde dehydrogenase inhibition as a pathogenic mechanism in Parkinson disease. Proc Natl Acad Sci U S A 110(2), 636–641. 10.1073/pnas.1220399110 [PubMed: 23267077]

Follmer C, Coelho-Cerqueira E, Yatabe-Franco DY, Araujo GD, Pinheiro AS, Domont GB and Eliezer D (2015). Oligomerization and Membrane-Binding Properties of Covalent Adducts Formed by the Interaction of Alpha-Synuclein with the Toxic Dopamine Metabolite 3,4-Dihydroxyphenylacetaldehyde (DOPAL). J Biol Chem. 10.1074/jbc.M115.686584

Follmer C, Romao L, Einsiedler CM, Porto TC, Lara FA, Moncores M, Weissmuller G, Lashuel HA, Lansbury P, Neto VM, Silva JL and Foguel D (2007). Dopamine affects the stability, hydration, and packing of protofibrils and fibrils of the wild type and variants of alpha-synuclein. Biochemistry 46(2), 472–482. 10.1021/bi061871+ [PubMed: 17209557]

Forno LS (1996). Neuropathology of Parkinson's disease. J Neuropathol Exp Neurol 55(3), 259–272. [PubMed: 8786384]

Gallegos S, Pacheco C, Peters C, Opazo CM and Aguayo LG (2015). Features of alpha-synuclein that could explain the progression and irreversibility of Parkinson's disease. Front Neurosci 9, 59 10.3389/fnins.2015.00059 [PubMed: 25805964]

Galvin JE (2006). Interaction of alpha-synuclein and dopamine metabolites in the pathogenesis of Parkinson's disease: a case for the selective vulnerability of the substantia nigra. Acta Neuropathol 112(2), 115–126. 10.1007/s00401-006-0096-2 [PubMed: 16791599]

Garrido-Maraver J, Cordero MD, Oropesa-Avila M, Fernandez Vega A, de la Mata M, Delgado Pavon A, de Miguel M, Perez Calero C, Villanueva Paz M, Cotan D and Sanchez-Alcazar JA (2014). Coenzyme q10 therapy. Mol Syndromol 5(3-4), 187–197. 10.1159/000360101 [PubMed: 25126052]

Glaser CB, Yamin G, Uversky VN and Fink AL (2005). Methionine oxidation, alpha-synuclein and Parkinson's disease. Biochim Biophys Acta 1703(2), 157–169. 10.1016/j.bbapap.2004.10.008 [PubMed: 15680224]

Goldstein DS, Sullivan P, Cooney A, Jinsmaa Y, Sullivan R, Gross DJ, Holmes C, Kopin IJ and Sharabi Y (2012). Vesicular uptake blockade generates the toxic dopamine metabolite 3,4-dihydroxyphenylacetaldehyde in PC12 cells: relevance to the pathogenesis of Parkinson's disease. J Neurochem 123(6), 932–943. 10.1111/j.1471-4159.2012.07924.x [PubMed: 22906103]

Goldstein DS, Sullivan P, Holmes C, Kopin IJ, Basile MJ and Mash DC (2011). Catechols in post-mortem brain of patients with Parkinson disease. Eur J Neurol 18(5), 703–710. 10.1111/j.1468-1331.2010.03246.x [PubMed: 21073636]

Goldstein DS, Sullivan P, Holmes C, Miller GW, Alter S, Strong R, Mash DC, Kopin IJ and Sharabi Y (2013). Determinants of buildup of the toxic dopamine metabolite DOPAL in Parkinson's disease. J Neurochem 126(5), 591–603. 10.1111/jnc.12345 [PubMed: 23786406]

Gonzalez-Burgos E, Fernandez-Moriano C, Lozano R, Iglesias I and Gomez-Serranillos MP (2017). Ginsenosides Rd and Re co-treatments improve rotenone-induced oxidative stress and mitochondrial impairment in SH-SY5Y neuroblastoma cells. Food Chem Toxicol 109(Pt 1), 38–47. 10.1016/j.fct.2017.08.013 [PubMed: 28843595]

Grunewald A, Kumar KR and Sue CM (2018). New insights into the complex role of mitochondria in Parkinson's disease. Prog Neurobiol. 10.1016/j.pneurobio.2018.09.003

Helley MP, Pinnell J, Sportelli C and Tieu K (2017). Mitochondria: A Common Target for Genetic Mutations and Environmental Toxicants in Parkinson's Disease. Front Genet 8, 177 10.3389/fgene.2017.00177 [PubMed: 29204154]

Hong M, Song KD, Lee HK, Yi S, Lee YS, Heo TH, Jun HS and Kim SJ (2016). Fibrates inhibit the apoptosis of Batten disease lymphoblast cells via autophagy recovery and regulation of mitochondrial membrane potential. In Vitro Cell Dev Biol Anim 52(3), 349–355. 10.1007/s11626-015-9979-7 [PubMed: 26659390]

Houlden H and Singleton AB (2012). The genetics and neuropathology of Parkinson's disease. Acta Neuropathol 124(3), 325–338. 10.1007/s00401-012-1013-5 [PubMed: 22806825]

Huang C, Ren G, Zhou H and Wang CC (2005). A new method for purification of recombinant human alpha-synuclein in Escherichia coli. Protein Expr Purif 42(1), 173–177. 10.1016/j.pep.2005.02.014 [PubMed: 15939304]

Joshi AU and Mochly-Rosen D (2018). Mortal engines: Mitochondrial bioenergetics and dysfunction in neurodegenerative diseases. Pharmacol Res 138, 2–15. 10.1016/j.phrs.2018.08.010 [PubMed: 30144530]

Kim H, Lee JY, Park KJ, Kim WH and Roh GS (2016). A mitochondrial division inhibitor, Mdivi-1, inhibits mitochondrial fragmentation and attenuates kainic acid-induced hippocampal cell death. BMC Neurosci 17(1), 33 10.1186/s12868-016-0270-y [PubMed: 27287829]

Kim S, Kim C and Park S (2017). Mdivi-1 Protects Adult Rat Hippocampal Neural Stem Cells against Palmitate-Induced Oxidative Stress and Apoptosis. Int J Mol Sci 18(9). 10.3390/ijms18091947

Kones R (2010). Parkinson's disease: mitochondrial molecular pathology, inflammation, statins, and therapeutic neuroprotective nutrition. Nutr Clin Pract 25(4), 371–389. 10.1177/0884533610373932 [PubMed: 20702843]

Kowalik-Jankowska T, Rajewska A, Jankowska E and Grzonka Z (2008). Products of Cu(II)-catalyzed oxidation of alpha-synuclein fragments containing M1-D2 and H50 residues in the presence of hydrogen peroxide. Dalton Trans (6), 832–838. 10.1039/b714440g

Kristal BS, Conway AD, Brown AM, Jain JC, Ulluci PA, Li SW and Burke WJ (2001). Selective dopaminergic vulnerability: 3,4-dihydroxyphenylacetaldehyde targets mitochondria. Free Radic Biol Med 30(8), 924–931. [PubMed: 11295535]

Krumschnabel G, Eigentler A, Fasching M and Gnaiger E (2014). Use of safranin for the assessment of mitochondrial membrane potential by high-resolution respirometry and fluorometry. Methods Enzymol 542, 163–181. 10.1016/B978-0-12-416618-9.00009-1 [PubMed: 24862266]

Lemasters JJ (1999). V. Necrapoptosis and the mitochondrial permeability transition: shared pathways to necrosis and apoptosis. Am J Physiol 276(1), G1–6. 10.1152/ajpgi.1999.276.1.G1 [PubMed: 9886971]

Leung KW, Yung KK, Mak NK, Chan YS, Fan TP and Wong RN (2007). Neuroprotective effects of ginsenoside-Rg1 in primary nigral neurons against rotenone toxicity. Neuropharmacology 52(3), 827–835. 10.1016/j.neuropharm.2006.10.001 [PubMed: 17123556]

Li SW, Lin TS, Minteer S and Burke WJ (2001). 3,4-Dihydroxyphenylacetaldehyde and hydrogen peroxide generate a hydroxyl radical: possible role in Parkinson's disease pathogenesis. Brain Res Mol Brain Res 93(1), 1–7. [PubMed: 11532332]

Liu Y, Zhang RY, Zhao J, Dong Z, Feng DY, Wu R, Shi M and Zhao G (2015). Ginsenoside Rd Protects SH-SY5Y Cells against 1-Methyl-4-phenylpyridinium Induced Injury. Int J Mol Sci 16(7), 14395–14408. 10.3390/ijms160714395 [PubMed: 26114390]

Lorenzen N, Lemminger L, Pedersen JN, Nielsen SB and Otzen DE (2014). The N-terminus of alpha-synuclein is essential for both monomeric and oligomeric interactions with membranes. FEBS Lett 588(3), 497–502. 10.1016/j.febslet.2013.12.015 [PubMed: 24374342]

Ludtmann MHR, Angelova PR, Horrocks MH, Choi ML, Rodrigues M, Baev AY, Berezhnov AV, Yao Z, Little D, Banushi B, Al-Menhali AS, Ranasinghe RT, Whiten DR, Yapom R, Dolt KS, Devine MJ, Gissen P, Kunath T, Jaganjac M, Pavlov EV, Klenerman D, Abramov AY and Gandhi S (2018). alpha-synuclein oligomers interact with ATP synthase and open the permeability transition

pore in Parkinson's disease. Nat Commun 9(1), 2293 10.1038/s41467-018-04422-2 [PubMed: 29895861]

Luth ES, Bartels T, Dettmer U, Kim NC and Selkoe DJ (2015). Purification of alpha-synuclein from human brain reveals an instability of endogenous multimers as the protein approaches purity. Biochemistry 54(2), 279–292. 10.1021/bi501188a [PubMed: 25490121]

Luth ES, Stavrovskaya IG, Bartels T, Kristal BS and Selkoe DJ (2014). Soluble, prefibrillar alpha-synuclein oligomers promote complex I-dependent, Ca2+-induced mitochondrial dysfunction. J Biol Chem 289(31), 21490–21507. 10.1074/jbc.M113.545749 [PubMed: 24942732]

Mahdaviani K, Benador IY, Su S, Gharakhanian RA, Stiles L, Trudeau KM, Cardamone M, Enriquez-Zarralanga V, Ritou E, Aprahamian T, Oliveira MF, Corkey BE, Perissi V, Liesa M and Shirihai OS (2017). Mfn2 deletion in brown adipose tissue protects from insulin resistance and impairs thermogenesis. EMBO Rep 18(7), 1123–1138. 10.15252/embr.201643827 [PubMed: 28539390]

Mahul-Mellier AL, Vercruysse F, Maco B, Ait-Bouziad N, De Roo M, Muller D and Lashuel HA (2015). Fibril growth and seeding capacity play key roles in alpha-synuclein-mediated apoptotic cell death. Cell Death Differ. 22(12), 2107–2122. 10.1038/cdd.2015.79 [PubMed: 26138444]

Manczak M, Kandimalla R, Yin X and Reddy PH (2019). Mitochondrial division inhibitor 1 reduces dynamin-related protein 1 and mitochondrial fission activity. Hum Mol Genet 28(2), 177–199. 10.1093/hmg/ddy335 [PubMed: 30239719]

Mazzulli JR, Mishizen AJ, Giasson BI, Lynch DR, Thomas SA, Nakashima A, Nagatsu T, Ota A and Ischiropoulos H (2006). Cytosolic catechols inhibit alpha-synuclein aggregation and facilitate the formation of intracellular soluble oligomeric intermediates. J Neurosci 26(39), 10068–10078. 10.1523/JNEUROSCI.0896-06.2006 [PubMed: 17005870]

Mor DE, Daniels MJ and Ischiropoulos H (2019). The usual suspects, dopamine and alpha-synuclein, conspire to cause neurodegeneration. Mov Disord 34(2), 167–179. 10.1002/mds.27607 [PubMed: 30633814]

Mor DE and Ischiropoulos H (2018). The Convergence of Dopamine and alpha-Synuclein: Implications for Parkinson's Disease. J Exp Neurosci 12, 1179069518761360. 10.1177/1179069518761360

Nakajima Y, Inokuchi Y, Nishi M, Shimazawa M, Otsubo K and Hara H (2008). Coenzyme Q10 protects retinal cells against oxidative stress in vitro and in vivo. Brain Res 1226, 226–233. 10.1016/j.brainres.2008.06.026 [PubMed: 18598676]

Norris EH, Giasson BI, Hodara R, Xu S, Trojanowski JQ, Ischiropoulos H and Lee VM (2005). Reversible inhibition of alpha-synuclein fibrillization by dopaminochrome-mediated conformational alterations. J Biol Chem 280(22), 21212–21219. 10.1074/jbc.M412621200 [PubMed: 15817478]

Pacheco CR, Morales CN, Ramirez AE, Munoz FJ, Gallegos SS, Caviedes PA, Aguayo LG and Opazo CM (2015). Extracellular alpha-synuclein alters synaptic transmission in brain neurons by perforating the neuronal plasma membrane. J Neurochem 132(6), 731–741. 10.1111/jnc.13060 [PubMed: 25669123]

Paik SR, Shin HJ and Lee JH (2000). Metal-catalyzed oxidation of alpha-synuclein in the presence of Copper(II) and hydrogen peroxide. Arch Biochem Biophys 378(2), 269–277. 10.1006/abbi.2000.1822 [PubMed: 10860544]

Panneton WM, Kumar VB, Gan Q, Burke WJ and Galvin JE (2010). The neurotoxicity of DOPAL: behavioral and stereological evidence for its role in Parkinson disease pathogenesis. PLoS One 5(12), e15251 10.1371/journal.pone.0015251 [PubMed: 21179455]

Parihar MS, Parihar A, Fujita M, Hashimoto M and Ghafourifar P (2008). Mitochondrial association of alpha-synuclein causes oxidative stress. Cell Mol Life Sci 65(7-8), 1272–1284. [PubMed: 18322646]

Paslawski W, Andreasen M, Nielsen SB, Lorenzen N, Thomsen K, Kaspersen JD, Pedersen JS and Otzen DE (2014). High stability and cooperative unfolding of alpha-synuclein oligomers. Biochemistry 53(39), 6252–6263. 10.1021/bi5007833 [PubMed: 25216651]

Peelaerts W, Bousset L, Van der Perren A, Moskalyuk A, Pulizzi R, Giugliano M, Van den Haute C, Melki R and Baekelandt V (2015). alpha-Synuclein strains cause distinct synucleinopathies after

local and systemic administration. Nature 522(7556), 340–344. 10.1038/nature14547 [PubMed: 26061766]

Plotegher N, Berti G, Ferrari E, Tessari I, Zanetti M, Lunelli L, Greggio E, Bisaglia M, Veronesi M, Girotto S, Dalla Serra M, Perego C, Casella L and Bubacco L (2017). DOPAL derived alpha-synuclein oligomers impair synaptic vesicles physiological function. Sci Rep 7, 40699 10.1038/srep40699 [PubMed: 28084443]

Post MR, Lieberman OJ and Mosharov EV (2018). Can Interactions Between alpha-Synuclein, Dopamine and Calcium Explain Selective Neurodegeneration in Parkinson's Disease? Front Neurosci 12, 161 10.3389/fnins.2018.00161 [PubMed: 29593491]

Rees JN, Florang VR, Eckert LL and Doorn JA (2009). Protein reactivity of 3,4-dihydroxyphenylacetaldehyde, a toxic dopamine metabolite, is dependent on both the aldehyde and the catechol. Chem Res Toxicol 22(7), 1256–1263. 10.1021/tx9000557 [PubMed: 19537779]

Roberts HL and Brown DR (2015). Seeking a Mechanism for the Toxicity of Oligomeric alpha-Synuclein. Biomolecules 5(2), 282–305. 10.3390/biom5020282 [PubMed: 25816357]

Rogers GW, Brand MD, Petrosyan S, Ashok D, Elorza AA, Ferrick DA and Murphy AN (2011). High throughput microplate respiratory measurements using minimal quantities of isolated mitochondria. PLoS One 6(7), e21746 10.1371/journal.pone.0021746 [PubMed: 21799747]

Rostovtseva TK, Gurnev PA, Protchenko O, Hoogerheide DP, Yap TL, Philpott CC, Lee JC and Bezrukov SM (2015). alpha-Synuclein Shows High Affinity Interaction with Voltage-dependent Anion Channel, Suggesting Mechanisms of Mitochondrial Regulation and Toxicity in Parkinson Disease. J Biol Chem 290(30), 18467–18477. 10.1074/jbc.M115.641746 [PubMed: 26055708]

Roychaudhuri R, Yang M, Deshpande A, Cole GM, Frautschy S, Lomakin A, Benedek GB and Teplow DB (2013). C-terminal turn stability determines assembly differences between Abeta40 and Abeta42. J Mol Biol 425(2), 292–308. 10.1016/j.jmb.2012.11.006 [PubMed: 23154165]

Sarafian TA, Littlejohn K, Yuan S, Fernandez C, Cilluffo M, Koo BK, Whitelegge JP and Watson JB (2017). Stimulation of synaptoneurosome glutamate release by monomeric and fibrillated alpha-synuclein. J Neurosci Res 95(9), 1871–1887. 10.1002/jnr.24024 [PubMed: 28117497]

Sarafian TA, Ryan CM, Souda P, Masliah E, Kar UK, Vinters HV, Mathern GW, Faull KF, Whitelegge JP and Watson JB (2013). Impairment of mitochondria in adult mouse brain overexpressing predominantly full-length, N-terminally acetylated human alpha-synuclein. PLoS One 8(5), e63557 10.1371/journal.pone.0063557 [PubMed: 23667637]

Schapira AH, Cooper JM, Dexter D, Clark JB, Jenner P and Marsden CD (1990). Mitochondrial complex I deficiency in Parkinson's disease. J Neurochem 54(3), 823–827. [PubMed: 2154550]

Smith G and Gallo G (2017). To mdivi-1 or not to mdivi-1: Is that the question? Dev Neurobiol 77(11), 1260–1268. 10.1002/dneu.22519 [PubMed: 28842943]

Staub RE, Quistad GB and Casida JE (1999). S-methyl N-butylthiocarbamate sulfoxide: selective carbamoylating agent for mouse mitochondrial aldehyde dehydrogenase. Biochem Pharmacol 58(9), 1467–1473. [PubMed: 10513990]

Stokes AH, Hastings TG and Vrana KE (1999). Cytotoxic and genotoxic potential of dopamine. J Neurosci Res 55(6), 659–665. 10.1002/(SICI)1097-4547(19990315)55:6<659::AID-JNR1>3.0.CO;2-C [PubMed: 10220107]

Subramaniam SR, Vergnes L, Franich NR, Reue K and Chesselet MF (2014). Region specific mitochondrial impairment in mice with widespread overexpression of alpha-synuclein. Neurobiol Dis 70, 204–213. 10.1016/j.nbd.2014.06.017 [PubMed: 25016198]

Tran TV, Shin EJ, Dang DK, Ko SK, Jeong JH, Nah SY, Jang CG, Lee YJ, Toriumi K, Nabeshima T and Kim HC (2017). Ginsenoside Re protects against phencyclidine-induced behavioral changes and mitochondrial dysfunction via interactive modulation of glutathione peroxidase-1 and NADPH oxidase in the dorsolateral cortex of mice. Food Chem Toxicol 110, 300–315. 10.1016/j.fct.2017.10.019 [PubMed: 29037473]

Tsang SH, Woodruff ML, Hsu CW, Naumann MC, Cilluffo M, Tosi J and Lin CS (2011). Function of the asparagine 74 residue of the inhibitory gamma-subunit of retinal rod cGMP-phophodiesterase (PDE) in vivo. Cell Signal 23(10), 1584–1589. 10.1016/j.cellsig.2011.05.007 [PubMed: 21616145]

Villalba JM, Parrado C, Santos-Gonzalez M and Alcain FJ (2010). Therapeutic use of coenzyme Q10 and coenzyme Q10-related compounds and formulations. Expert Opin Investig Drugs 19(4), 535–554. 10.1517/13543781003727495

Villar-Pique A, da Fonseca TL and Outeiro TF (2015). Structure, function and toxicity of alpha-synuclein: the Bermuda triangle in synucleinopathies. J Neurochem. 139, 240–255. 10.1111/jnc.13249 [PubMed: 26190401]

Watson JB, Hatami A, David H, Masliah E, Roberts K, Evans CE and Levine MS (2009). Alterations in corticostriatal synaptic plasticity in mice overexpressing human alpha-synuclein. Neuroscience 159(2), 501–513. 10.1016/j.neuroscience.2009.01.021 [PubMed: 19361478]

Werner-Allen JW, DuMond JF, Levine RL and Bax A (2016). Toxic Dopamine Metabolite DOPAL Forms an Unexpected Dicatechol Pyrrole Adduct with Lysines of alpha-Synuclein. Angew Chem Int Ed Engl 55(26), 7374–7378. 10.1002/anie.201600277 [PubMed: 27158766]

Werner-Allen JW, Levine RL and Bax A (2017). Superoxide is the critical driver of DOPAL autoxidation, lysyl adduct formation, and crosslinking of alpha-synuclein. Biochem Biophys Res Commun. 10.1016/j.bbrc.2017.04.050

Werner-Allen JW, Monti S, DuMond JF, Levine RL and Bax A (2018). Isoindole Linkages Provide a Pathway for DOPAL-Mediated Cross-Linking of alpha-Synuclein. Biochemistry 57(9), 1462–1474. 10.1021/acs.biochem.7b01164 [PubMed: 29394048]

Winner B, Jappelli R, Maji SK, Desplats PA, Boyer L, Aigner S, Hetzer C, Loher T, Vilar M, Campioni S, Tzitzilonis C, Soragni A, Jessberger S, Mira H, Consiglio A, Pham E, Masliah E, Gage FH and Riek R (2011). In vivo demonstration that alpha-synuclein oligomers are toxic. Proc Natl Acad Sci U S A 108(10), 4194–4199. 10.1073/pnas.1100976108 [PubMed: 21325059]

Youdim MB and Riederer P (1997). Understanding Parkinson's disease. Sci Am 276(1), 52–59. [PubMed: 8972618]

Zhang YL, Liu Y, Kang XP, Dou CY, Zhuo RG, Huang SQ, Peng L and Wen L (2018). Ginsenoside Rb1 confers neuroprotection via promotion of glutamate transporters in a mouse model of Parkinson's disease. Neuropharmacology 131, 223–237. 10.1016/j.neuropharm.2017.12.012 [PubMed: 29241654]

Zhou W, Long C, Reaney SH, Di Monte DA, Fink AL and Uversky VN (2010). Methionine oxidation stabilizes non-toxic oligomers of alpha-synuclein through strengthening the auto-inhibitory intra-molecular long-range interactions. Biochim Biophys Acta 1802(3), 322–330. 10.1016/j.bbadis.2009.12.004 [PubMed: 20026206]

SIGIFICANCE STATEMENT

Along with deficits in dopamine metabolism, mitochondrial impairment remains a major area of research focus in Parkinson's disease. The current study showed that the dopamine metabolite, 3,4-dihydroxyphenyl-acetaldehyde (DOPAL), enhanced oligomerization of α-synuclein, which inhibited mitochondrial function and was rescued by multiple small molecules.

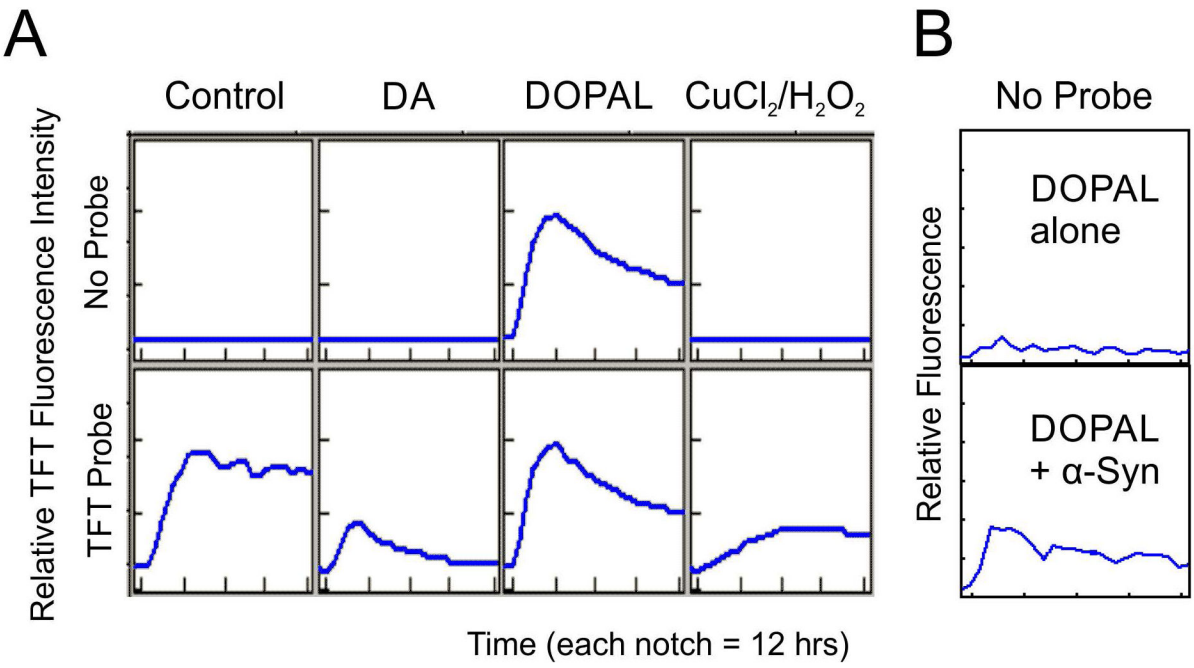

Figure 1.

A. Fibrillation profiles for recombinant α-Syn. Incubations were performed in 96 well plates with constant agitation for 48 hr measuring green fluorescence (E_x=485, E_m=538) at 2 hr intervals (Sarafian et al., 2017) in the absence (top-panels, no probe) or presence of 40 μM thioflavin T (bottom panels, TFT probe). Fibrillations contained: buffer only (control), 200 μM dopamine (DA), 400 μM DOPAL, 50 μM $CuCl_2$/1 mM H_2O_2. Fibrillations were repeated 4 times with similar results using different preparations of recombinant α-synuclein protein. N.B. Fluorescence observed in DOPAL top panel in the absence of TFT probe likely reflects DOPAL-conjugated to aggregated α-Syn (Coelho-Cerqueira et al., 2014). **B.** DOPAL alone (top panel) shows little or no endogenous fluorescence relative to aggregated DOPAL/α-Syn (bottom panel). This was a separate experiment from panel A in the absence of the TFT probe.

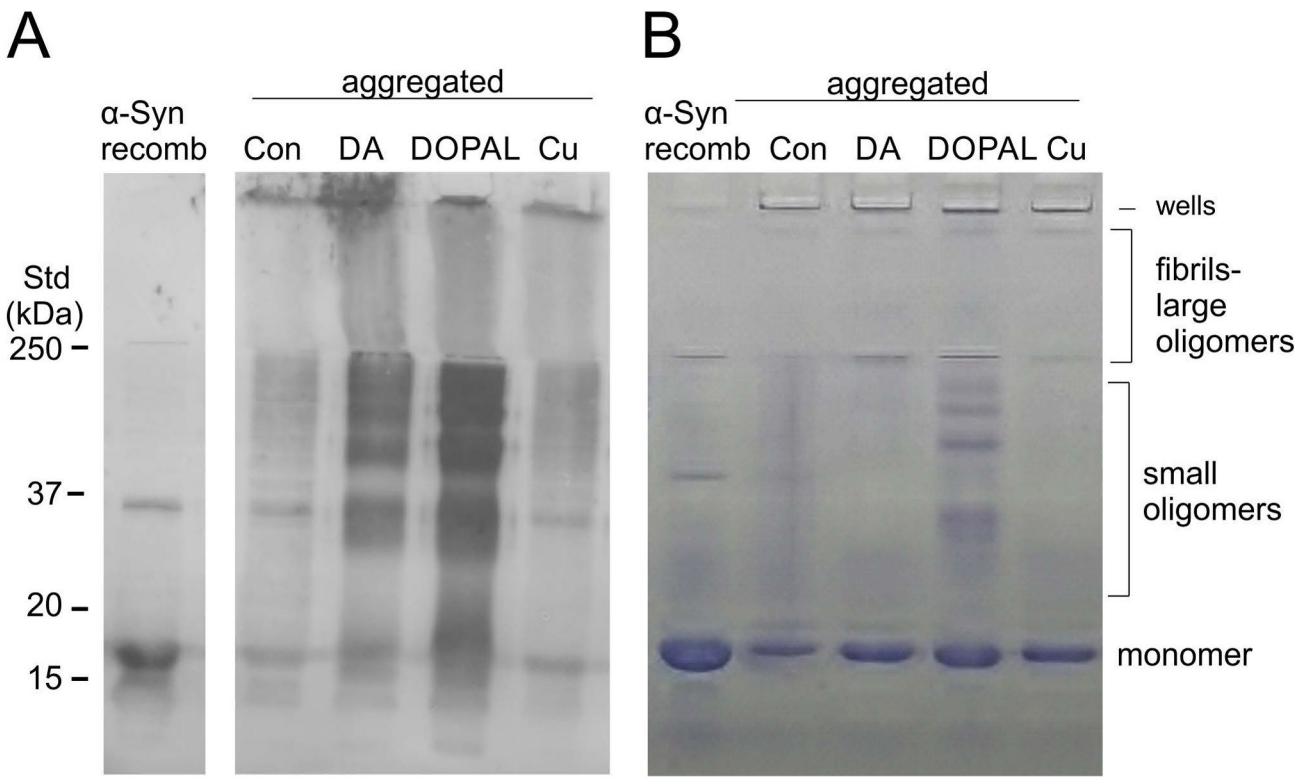

Figure 2.

Immunoblotting and SDS-PAGE analyses of monomeric and fibrillated α-Syn. **A.** Western immunoblot was stained with α-synuclein monoclonal antibody. Lanes: α-Syn recombinant monomeric protein (α-Syn recomb); Con, untreated aggregated; DA, dopamine-aggregated; DOPAL-aggregated; $CuCl_2/H_2O_2$ (Cu) aggregated. Samples were not subjected to Zeba column purification. Zeba columns do not alter monomer or oligomer banding patterns but substantially diminish all bands from untreated control aggregated α-synuclein (data not shown). The locations of monomers and likely small/large oligomers and fibrils are denoted. This experiment was repeated five times with similar results. **B.** SDS-PAGE gel was stained with Coomassie Brilliant Blue R250. The same samples in Panel A were loaded in identical lanes. Analyses were repeated three times with similar results.

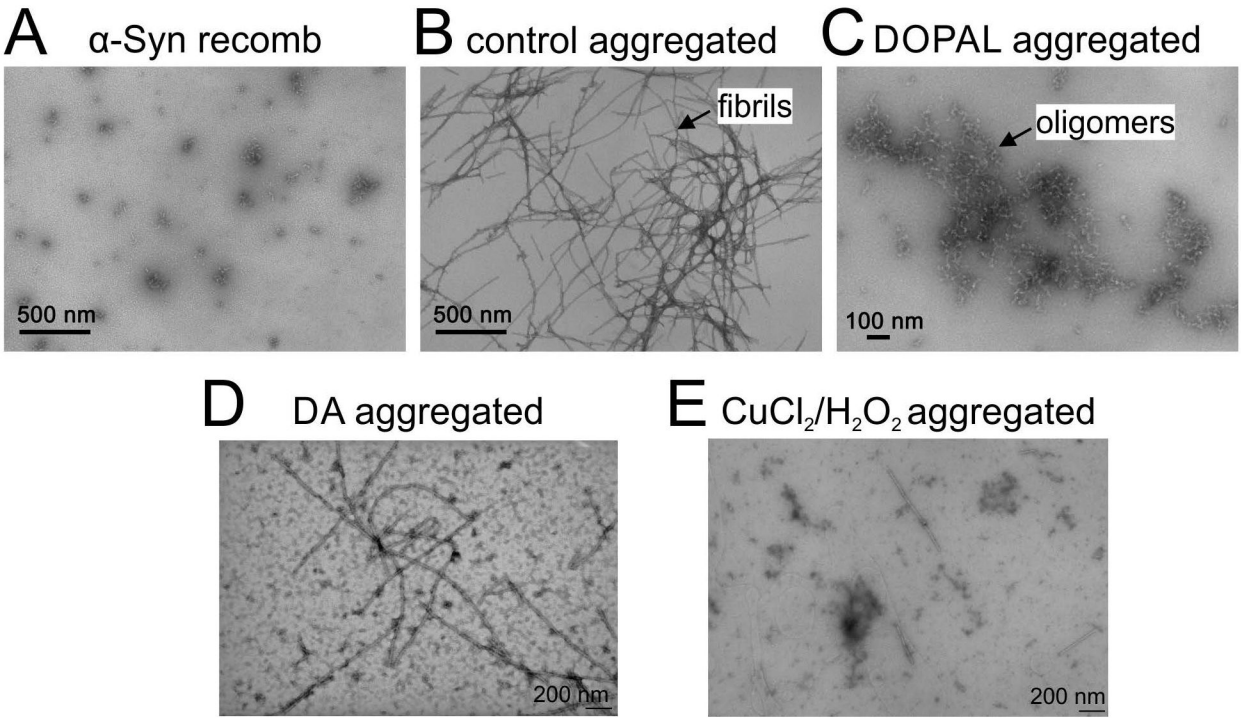

Figure 3.

Transmission electron microscopy (TEM) of monomeric and 48 hr fibrillated α-Syn. **A.** **N**on-fibrillated monomers (α-Syn recomb) **B.** Untreated control aggregated, fibrils are denoted by arrow **C.** DOPAL aggregated, arrow denotes DOS oligomers **D.** Dopamine (DA) aggregated **E.** $CuCl_2/H_2O_2$ aggregated. Scale bars are provided for each micrograph.

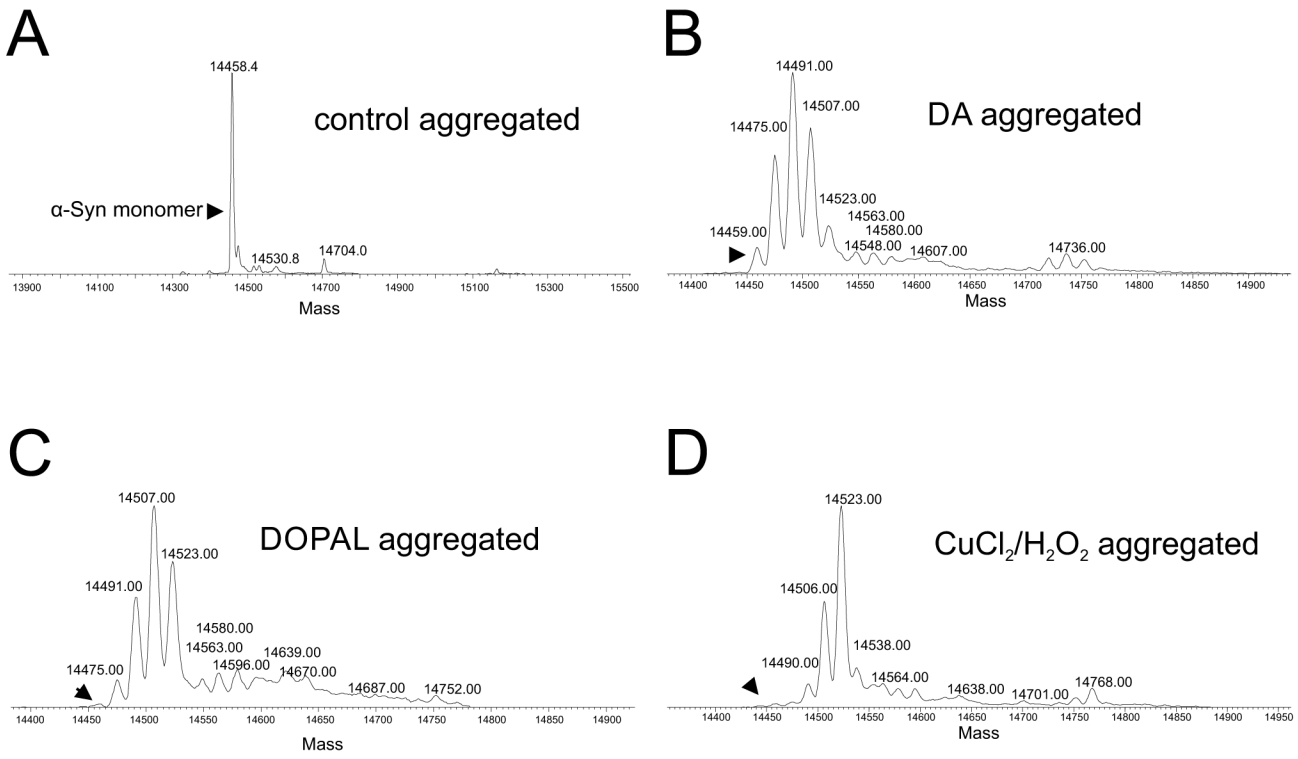

Figure 4.

Top-down, intact protein mass spectrometry (MS) of aggregated α-Syn proteoforms after 48 hours of fibrillation **A.** Untreated (control aggregated), **B.** Dopamine (DA) aggregated **C.** DOPAL aggregated **D.** $CuCl_2/H_2O_2$ aggregated. Samples were solubilized with formic acid and intact proteins were analyzed by top-down MS and resolved by liquid chromatography. Arrows point to unmodified monomer locations (14458.4 mass). Y-axis (not shown) was the relative intensity of the mass spectrometric signal on a linear scale.

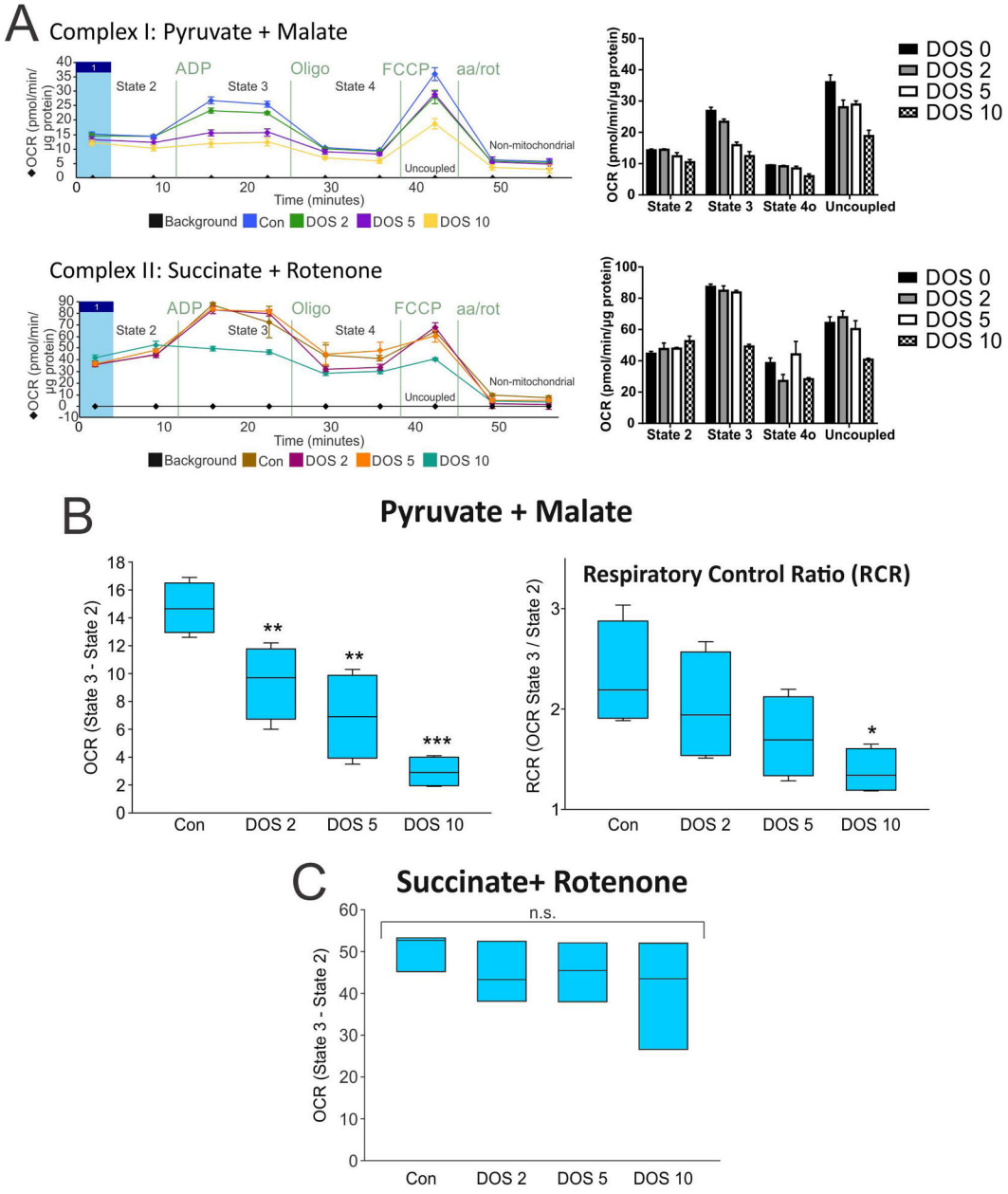

Figure 5.

Seahorse respiration analysis of DOS-treated mouse brain mitochondria. Mitochondria were incubated with DOS for 60 min at 30°C (DOS 0 = no protein; DOS 10 = 6.7 μM). Oxygen consumption rate (OCR) in the presence of either pyruvate + malate or succinate + rotenone was performed using an XF96 Extracellular Flux Analyzer (Agilent) as described in Materials and Methods (Rogers et al., 2011).

A. Time courses and bar graph summaries for either complex 1 (pyruvate + malate) or complex II (succinate + rotenone)-driven respiration are shown relative to DOS concentrations: Values represent means of 5 determinations ± SEM for a single, representative experiment. Sections (left panel) corresponding to State 2, State 3, State 4 along with Uncoupled and Non-mitochondrial respiration are indicated (Con: Control;

Oligo: oligomycin; FCCP: Carbonyl cyanide p-(trifluoromethoxy)phenylhydrazone; aa: antimycin A; rot: rotenone). N.B. All subsequent numbers for Statistical analysis (below) of the entire data set (N=4 experiments, 20 determinations, two mitochondrial preparations from two separate mice) are shown as the mean ± Standard Deviation (SD).

B. OCR values (State 3-State 2) for complex I/pyruvate + malate (left panel) are shown for increasing DOS amounts displayed as a Box-Whisker Plot with median (horizontal lines) and quarterly confidence intervals (vertical lines). The Respiratory Control Ratio (RCR, OCR State 3/State 2) for pyruvate + malate (right panel) is also shown as a Box-Whisker plot as a function of DOS concentrations.

C. OCR values (State 3-State 2) for complex II/succinate + rotenone (bottom panel) are shown for increasing DOS amounts.

Statistics:**Fig. 5B (left panel)** OCR: $F_{(3,15)}$= 18.3, N=4, p<0.001, DOS 10 (mean ± SD, 2.95 ± 1.11) vs Con (14.7 ± 1.84), Bonferroni post-hoc test, t=7.2,) *** p<0.001; post-hoc tests were also significant for DOS 2, * p<0.05 and DOS 5, ** p<0.01 (One Way ANOVA). Fig. 5B (right panel) RCR: $F_{(3,15)}$=3.8, N=4, p<0.05, DOS 10 (mean ± SD, 1.3 ± 0.24) vs Con (2.3 ± 0.52), Bonferroni post-hoc test, t=3.3, *p<0.05 (One Way ANOVA). Fig. 5C (bottom panel) $F_{(3, 14)}$=0.82, N=4, p=0.06, not significant (One Way ANOVA).

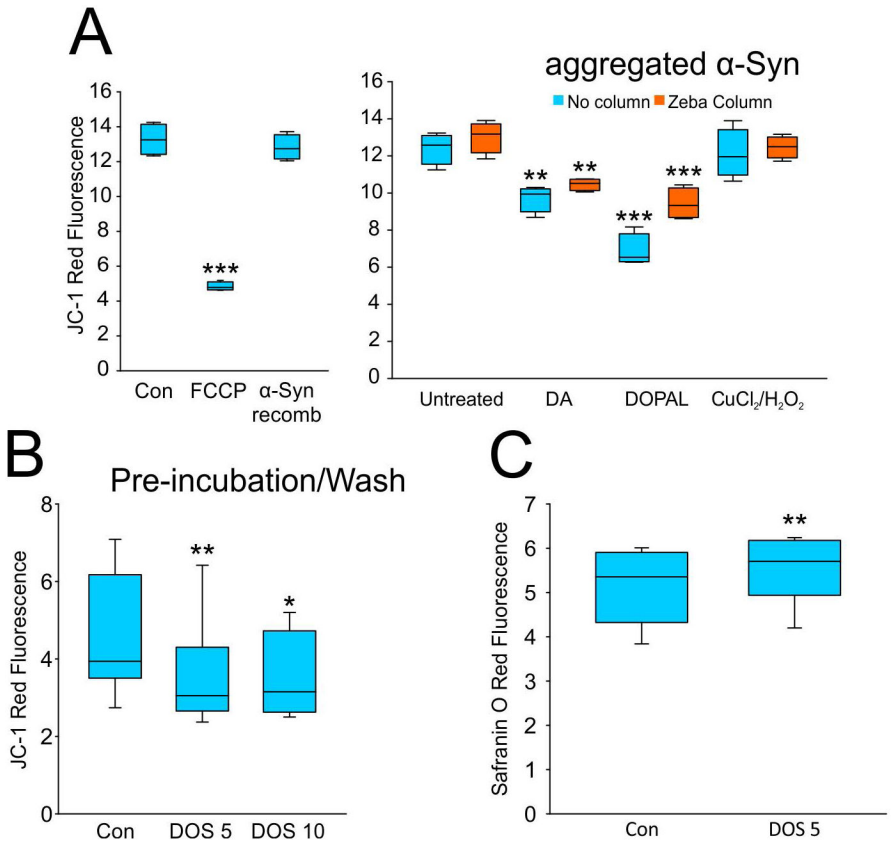

Figure 6.

Fluorescence assays for mitochondrial membrane potential.

A. Mitochondria (0.7 mg/ml) were exposed to buffer alone control (Con), FCCP, or an α-synuclein sample (α-Syn recomb, 4 μM) (left panel) for 15 min at room temp prior to transfer to JC-1 solutions in 96-well plates. In the right panel, aggregated α-Syn (3.4 μM), either untreated control (Con) or treated [dopamine (DA), DOPAL, $CuCl_2/H_2O_2$] were also incubated for 15 min at room temperature prior to transfer to JC-1 solutions in 96-well plates. Duplicate samples in the right panel were also purified over Zeba columns (orange) to remove free small compounds. Red fluorescence (E_x= 530, E_m=592) was measured after 30 minutes incubation in the dark at 37°C using a Fluoroskan Ascent FL plate reader. JC-1 fluorescence values are displayed as Box-Whisker Plots (N = 4 determinations, one mitochondrial preparation from a single mouse). Similar results were obtained in three additional mitochondrial preparations. ***Statistics:* Left panel**, $F_{(2,11)}$=78.3, N=4, p<0.001; FCCP (mean ± SD, 6.7± 0.25) vs Con (15.2 ± 0.91), Bonferroni post-hoc test, t= 11.6,*** p< 0.001(One-Way ANOVA**) Right panel**, $F_{(7,31)}$=24.6, N=4, p<0.001; DA + Zeba (mean ± SD, 10.5 ± 0.32) vs untreated control + Zeba (13.0 ± 0.86), **p<0.01 Bonferroni post-hoc test; DOPAL + Zeba column (9.4 ± 0.84) vs untreated control + Zeba (13.0 ± 0.86) ***p<0.001 Bonferroni post-hoc test (One Way ANOVA).

B. Mitochondria were incubated with either DOS 5 or DOS 10 (6.7 μM) for 30 min at 30°C followed by centrifugation and washing with buffer to remove free DOS as described in Materials and Methods. JC-1 fluorescence values are represented as Box-Whisker Plots [N =

4-8 determinations, mean ± SD, one mouse mitochondrial preparation, Con (4.6 ± 1.6); DOS 5 (3.53 ± 1.4); DOS 10 (3.5 ± 1.18) *, p<0.05, **p < 0.01, Paired-*t* test]

C. Mitochondrial membrane potential assay using Safranin O Red fluorescence. Mitochondria were pre-incubated with DOS 5 and washed thoroughly. Values represent means of 8-9 determinations ± SD using mitochondrial preparations from 4 separate mice [mean ± SD, DOS 5 (5.5 ±0.76) vs Con (5.2 ± 0.83), ** p < 0.01 Paired *t*-test].

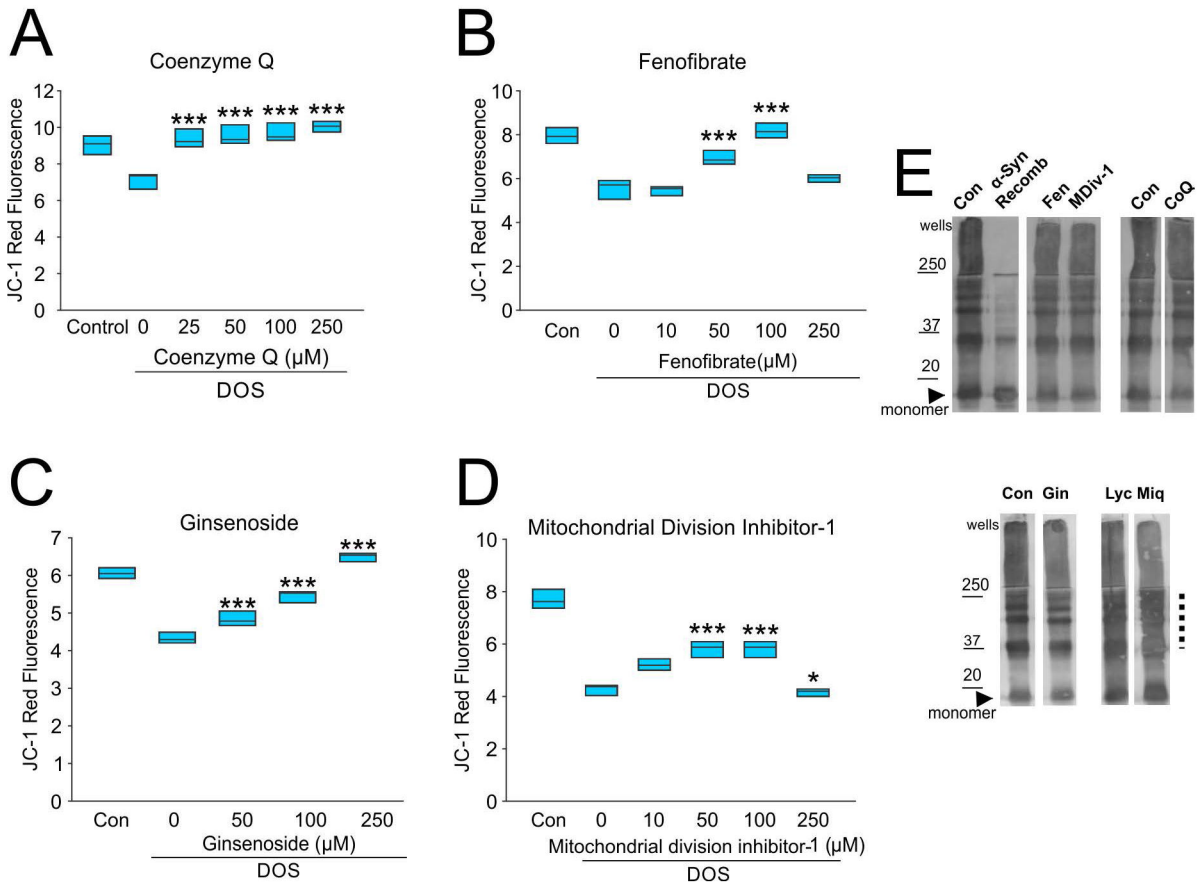

Figure 7.

Protective effects of four compounds against DOS-induced decrease in mitochondrial membrane potential measured with JC-1: **A** (Coenzyme Q10), **B** (Fenofibrate), **C** (Ginsenoside Re), **D** (Mitochondrial division inhibitor-1). Mitochondria were treated with each compound for 15 mins at room temperature followed by 15 min treatment with DOS 5 (3.4 μM). JC-1 fluorescence values are displayed as Box-Whisker Plots. Values represent means of four determinations ± SD from individual experiments from mitochondrial preparations from multiple mice. Experiments were repeated 3 times with similar results. **Statistics:** Coenzyme Q10, $F_{(4,19)}$=20.7, N=4, p<0.001; Fenofibrate, $F_{(4,19)}$= 44.8, N=4, p<0.001; Ginsenoside Re, $F_{(4,19)}$=112.7, N=4, p<0.001; Mitochondrial division inhibitor-1, $F_{(4,19)}$ = 39.7, N=4, p<0.001. Fisher LSD post-hoc test values are denoted as *p<0.05 ** p<0.01 *** p<0.001.

E. Western blot analysis of the effect of several compounds on protein banding patterns of DOS. Stacking gel blots (top) were included with resolving gels. Arrows denote location of monomers. Dotted line denotes location of smeared bands corresponding to likely modified small oligomers (bottom panel). DOS samples were incubated with compounds (250 μM) for 24 hrs at 37°C. Con: untreated control DOS; Recomb α-Syn, monomeric recombinant α-synuclein; Fen, Fenofibrate; Mdiv-1, Mitochondrial division inhibitor-1; CoQ10, Coenzyme Q10; Gin: Ginsenoside Re, Lyc: lycopene; Miq, Mitoquinone.

Table 1.

List of small molecules (39 total) tested for mitochondrial protection against DOS. Protection (red) is denoted by +; inhibition is denoted by −; no effect is denoted by 0. Compounds were purchased commercially from either MilliporeSigma (MS), MedChemExpress (MCE), or European Pharmacopoeia Reference Standards/ Chemical Reference Standards (CRS). Note well: The threshold for protection (+) was > 10% relative to an untreated DOS control for a given compound. Each compound was tested once except positive blockers (Coenzyme Q10, Ginsenoside Re, Fenofibrate, Mitochondrial Division Inhibitor −1), which were further tested in dose response experiments in Figure 7.

Name	Source	Protection	Name	Source	Protection
Adenosine triphosphate	MS	0	Kaempferol	MS	−
Ascorbic Acid	MCE	0	Lipoic Acid	MCE	0
Butylated hydroxyanisole	MS	0	Lutein	MS	0
Caffeic acid phenethyl ester	MCE	−	Lycopene	MCE	−
Caffeine	MS	0	Melatonin	MS	0
Carnosic Acid	MS	−	Mitochondrial Division Inhibitor-1	MS	+
Coenzyme Q10	MS	+	Mitoquinone	MCE	−
Creatine	MS	0	N-Acetylcysteine	MCE	0
Curcumin	MS	0	N-acetylsalicylic acid	MS	0
Cyclosporine A	MS	0	Nicotinamide adenine dinucleotide	MS	0
Deferoxamine	MS	0	Osthole	MCE	0
Dexamethazone	MS	0	Palmitelaidic Acid	MCE	−
Dimeton	MS	0	PD 168316	MS	−
Echincoside	MCE	0	Piperine	MCE	0
Edavarone	MS	0	Protocatechuic acid	MCE	−
Epigallocatechin Gallate	MS	0	Quercetin	MS	−
Fenofibrate	MS	+	Resveratrol	MS	−
Ginsenoside Rb1	CRS	0	Tannic Acid	MS	−
Ginsenoside Re	MCE	+	Zeoxanthin	MS	0
Hesperidin	MCE	0			